Targeting heme oxygenase-1 dependency in SMARCA4-deficient cancers

Andrew Garnier

Department of Biochemistry

McGill University

February 2024

A thesis submitted to McGill University in partial fulfillment of the requirements of the degree of Master of Science.

ABSTRACT

Chromatin remodelers are frequently implicated with cancer, with the SWI/SNF family being the most frequently mutated in ~20% of cancers. Each SWI/SNF complex includes one of the two mutually exclusive ATPase subunits, SMARCA4 and SMARCA2. SMARCA4 has been found to be inactivated by mutations in ~100% of small cell carcinoma of the ovary, hypercalcemic type (SCCOHT), a rare and deadly cancer affecting young women, as well as other cancers such as non-small-cell lung carcinomas (NSCLCs; ~10%). SMARCA4-deficient cancers are highly resistant to conventional chemotherapies and remain hard to treat. Identification of new and effective treatment options is thus crucial to improve patient survival. Recently, our lab has identified heme metabolism to be a vulnerable target for SMARCA4-deficient cancers. One major contributor to heme metabolism is heme oxygenase-1 (HO-1), a heme-degrading enzyme. We hypothesize that targeting HO-1 will induce synthetic lethality in SMARCA4-deficient cancers and aim to determine the underlying molecular mechanisms while working towards uncovering potent inhibitors. Through genetic perturbation, our findings demonstrate the efficacy of HO-1 targeting for selective SMARCA4-deficient cell death, in part through heme-induced DNA damage. Currently, available HO-1 inhibitors are ineffective at selectively killing SMARCA4-deficient cancers due to their lack of either competitiveness with heme or HO-1 specificity. Thus, virtual screening through molecular docking of common drugs, natural products, and novel compounds with AutoDock Vina was used to find novel HO-1 inhibitors. The top validated candidates demonstrated a degree of selective efficacy, underscoring their promising potential. Together, this study demonstrates HO-1 as an effective target for SMARCA4-deficient cancer, while work remains to optimize HO-1 inhibitors to exploit HO-1 dependency in a clinical setting.

RÉSUMÉ

Les remodeleurs de la chromatine sont souvent impliqués dans le cancer, avec la famille SWI/SNF la plus fréquemment mutée, dans environ 20 % des cancers. Chaque complexe SWI/SNF inclut l'une des deux sous-unités ATPase de manière mutuellement exclusive, SMARCA4 et SMARCA2. SMARCA4 est inactivé par des mutations dans environ 100 % des carcinomes à petites cellules des ovaires de type hypercalcémique (SCCOHT), un cancer rare et mortel qui affecte les jeunes femmes, ainsi que dans d'autres cancers comme les carcinomes pulmonaires non à petites cellules (NSCLC; ~10 %). Les cancers déficients en SMARCA4 sont très résistants aux chimiothérapies conventionnelles et restent difficiles à traiter. Il est donc essentiel de trouver de nouvelles options thérapeutiques efficaces pour améliorer la survie des patients. Notre laboratoire a récemment identifié le métabolisme de l'hème comme une cible vulnérable pour les cancers déficients en SMARCA4. L'une des principales composantes du métabolisme de l'hème est l'hème oxygénase-1 (HO-1), une enzyme qui dégrade l'hème. Nous émettons l'hypothèse que le ciblage de HO-1 provoquera une létalité synthétique dans les cancers déficients en SMARCA4 et nous cherchons à déterminer les mécanismes moléculaires sous-jacents tout en travaillant à la découverte d'inhibiteurs puissants. Par le biais de perturbations génétiques, nos résultats démontrent l'efficacité du ciblage de HO-1 pour la mort sélective des cellules déficientes en SMARCA4 par dommages à l'ADN induits par l'hème. Les inhibiteurs de HO-1 disponibles sont inefficaces pour tuer sélectivement les cancers déficients en SMARCA4 en raison de leur manque de compétitivité avec l'hème ou de spécificité de HO-1. Le criblage virtuel par ancrage moléculaire de médicaments courants, de produits naturels, et de nouveaux composés avec AutoDock Vina a donc été utilisé pour trouver de nouveaux inhibiteurs. Les candidats les mieux validés ont démontré un certain degré d'efficacité sélective, ce qui souligne leur potentiel prometteur. L'ensemble de ces travaux

démontre que HO-1 est une cible efficace pour les cancers déficients en SMARCA4, mais il reste à identifier un inhibiteur efficace pour permettre d'exploiter pleinement cette vulnérabilité.

TABLE OF CONTENTS

ACKNOWLEDGEMENTS

First and foremost, I express my greatest appreciation to my supervisor, Dr. Sidong Huang. Under Sid's guidance, he allowed me the autonomy to shape my project and pursue my interests in research while providing unwavering support. Aside from research, Sid has been an incredible role model, demonstrating incredible curiosity, perseverance, and kindness. I am eternally thankful for the invaluable experience of working with him.

I am indebted to the remarkable individuals in my lab who have been supportive throughout my entire degree. They made the lab a fun and welcoming environment that I was excited to come to every day. Zheng was instrumental in my research, and I am extremely grateful for the time he spent training me to be a proficient researcher. Special recognition goes to Hannah and Paco for their generous time in answering my questions and assistance whenever needed.

I extend my sincere appreciation to my committee members, Dr. Natasha Chang and Dr. Martin Schmeing for their invaluable feedback. My gratitude extends to the Department of Biochemistry and the people within who have made my experience incredibly enjoyable. Additionally, the student associations and clubs at McGill I have been a part of during my studies have contributed significantly to my experience and fulfillment through graduate studies.

Thank you to all my friends and family who have stood by me during my academic journey. I especially want to recognize Evan, Matt, and Mason for their unwavering support and willingness to listen to my thoughts and musings. I am genuinely thankful to everyone, big or small, who has played a part in shaping the person I am today.

Finally, I acknowledge my funding sources, Canada Graduate Scholarship-Master's–CIHR and Master's Training Scholarship–FRQS, for providing financial support to conduct my research.

CONTRIBUTION OF AUTHORS

A.G. analyzed the data and wrote the thesis. S.H. provided substantial feedback. S.H., A.A., and H.H. provided editorial help on the thesis. A.G., Z.F., and S.H. designed the experiments. Z.F., initiated the project. A.G. performed all the experiments unless otherwise stated. Z.F. performed zinc protoporphyrin treatment assays.

LIST OF ABBREVIATIONS

BAF	BRG1/BRM-associated factor
BC	Bilirubin conjugate
BR	Bilirubin
BRG1	Brahma-related gene-1
BRM	Brahma homolog
BV	Biliverdin
BVR	Biliverdin reductase
CO	Carbon monoxide
COCONUT	Collection of Open Natural Products
CORM	Carbon monoxide-releasing molecule
CORM-2	Tricarbonyldichlororuthenium(II) dimer
EIF2AK1	Eukaryotic initiation factor 2-alpha kinase 1
ER	Endoplasmic reticulum
FDA	Food and Drug Administration
G4	G-quadruplex
HIF-1	Hypoxia-inducible factor 1
HO	Heme oxygenase

IC_{50}	Half maximal inhibitory concentration
IF	Immunofluorescence
Keap1	Kelch-like ECH-associated protein 1
NF-κB	Nuclear factor kappa B
Nrf2	Nuclear Factor Erythroid 2-Related Factor 2
NSCLC	Non-small cell lung cancer
PBS	Phosphate buffer saline
PDB	Protein Data Bank
ROS	Reactive oxygen species
SCCOHT	Small cell carcinoma of the ovary, hypercalcemic type
shRNA	Short hairpin RNA
SMARCA	SWI/SNF related, matrix associated, actin dependant regulator of chromatin
SWI/SNF	Switch/Sucrose non-fermentable
ZnPP	Zinc protoporphyrin

LIST OF FIGURES AND TABLES

INTRODUCTION

SMARCA4 and SMARCA4-deficient cancers

Cancer is a common and deadly disease; it is the second leading cause of death globally and the leading cause of death in Canada *(1, 2)*. As of 2023, it is estimated that 45% of Canadians will be diagnosed with cancer in their lifetime and 22% of Canadians will die from cancer *(3)*. At its core, cancer involves changes to or mutations in the DNA of our cells. These alterations disrupt the delicate balance that regulates cell growth and division. The two-dimensional structure of DNA and sequence is critical, but just as critical is how DNA is organized in three-dimensional space. DNA wraps around histones forming nucleosomes which are the building blocks of chromatin, a dynamic and adaptable complex. The arrangement of nucleosomes impacts the accessibility of binding sites for transcription factors, leading to alterations in gene expression and transcriptional activity *(4)*.

Influencing the arrangement of nucleosomes are chromatin remodeling complexes, resulting in adjustments to both chromatin architecture and gene expression. The SWI/SNF (Switch/Sucrose Non-Fermentable) family of chromatin remodeling complexes was first discovered in the 1980s by researchers studying gene regulation in yeast *(5, 6)*. They observed that certain genes were turned on or off by the chromatin-remodeling complex. Subsequently, the human homologous SWI/SNF complex was partially purified and showed ATP-dependent nucleosome mediation *(7)*. In the context of cancer, inactivating mutations in SWI/SNF complex subunits have been found to contribute to tumorigenesis *(8)*. Moreover, the SWI/SNF family of complexes is mutated in about 20% of all human cancers *(9)*. Each SWI/SNF complex includes one of the two mutually exclusive ATPase subunits, SMARCA4 and SMARCA2 (SWI/SNF-related, matrix-associated, actin-dependent regulator of chromatin). SMARCA4 (also known as

BRG1 (brahma-related gene-1)) and SMARCA2 (also known as BRM (brahma homolog)) share high sequence homology and have similar functions, although they may have distinct roles in specific cellular contexts *(10, 11)*. Additionally, in some contexts, SMARCA4 and SMARCA2 can compensate for the loss of the other in the SWI/SNF (also known as BAF (BRG1/BRM-associated factor)) complex *(12, 13)*. SMARCA4 and SMARCA2 utilize the energy derived from ATP hydrolysis to slide, eject, or restructure nucleosomes *(14)*. By doing so, they can expose or conceal specific gene regulatory elements, such as enhancers and promoters, and regulate the binding of transcription factors and other regulatory proteins to DNA *(14)*. The process of chromatin remodeling is crucial for various cellular processes, such as gene activation, repression, DNA replication, and DNA repair *(15)*.

SMARCA4 has been implicated in the maintenance of chromatin states during cellular differentiation and development, such as neural development, cardiac development, hematopoietic development, limb development, and organogenesis *(16-20)*. These studies emphasize that the proper functioning of SMARCA4 is vital for maintaining genomic stability and cell homeostasis. Thus, mutations or dysregulation of SMARCA4 can have significant implications for human health and disease. Most cancer types have been shown to exhibit heightened SMARCA4 expression levels, which were found to be associated with reduced overall survival in several instances *(21)*. In contrast, inactivating SMARCA4 mutations have been identified in certain cancers, such as ~10% of non-small cell lung cancer (NSCLC) and ~100% small cell carcinoma of the ovary, hypercalcemic type (SCCOHT), a rare and deadly cancer affecting young women *(22-25)*. Precisely, SCCOHT is characterized by the dual loss of SMARCA4 and SMARCA2 through mutations and epigenetic silencing, respectively *(26)*. SCCOHT has a simple genome making it ideal for studying SMARCA4 deficiency *(27)*.

SMARCA4-deficient cancers remain hard to treat as current treatment options are limited and conventional chemotherapy is ineffective. Specific challenges in treating SMARCA4-deficient cancers are caused by the essential function of the SWI/SNF complex, the numerous genetic and epigenetic alterations incurred, and the heterogeneity of disease *(22)*. SMARCA4-deficient cancers have attracted significant attention due to their distinct vulnerabilities, opening the possibility of exploiting synthetic lethal interactions for therapeutic purposes since loss of SMARCA4 is not directly druggable. Synthetic lethality refers to the phenomenon where the simultaneous presence of two genetic alterations leads to cell death, while individual mutations do not significantly affect cell viability *(28)*. Our aim is to leverage synthetic lethality to selectively target SMARCA4-deficient cancer cells while preserving the viability of SMARCA4-proficient normal cells.

Heme oxygenase-1 is a heme degrading enzyme

Our lab has previously determined heme metabolism to be a vulnerable target in SMARCA4-deficient cancers following a synthetic lethal shRNA screen (unpublished). Heme (iron protoporphyrin IX) is an iron coordinating complex. Heme serves as an essential prosthetic group for many proteins, named hemoproteins, where it plays an important role in gas transportation and sensing, catalysis, electron transfer, and can influence gene expression *(29)*. Iron can cycle between ferrous (Fe^{2+}) and ferric (Fe^{3+}) states, with ferric iron predominating within the cell *(30)*. Heme containing ferrous iron heme has toxic properties and can influence reactive oxygen species (ROS) production through the generation of hydroxyl radicals through the Fenton reaction between hydrogen peroxide and ferrous iron *(31, 32)*. The Fenton reaction is as follows:

$$Fe^{2+} + H_2O_2 \longrightarrow Fe^{3+} + HO\bullet + OH^- \qquad (33)$$

Other mechanisms of heme toxicity include lipid peroxidation, heme-induced endoplasmic reticulum (ER) stress, and DNA damage *(34-36)*. Thus, the cell needs to regulate heme levels in the cell. In the 1960s, it was discovered that there was an unknown substance metabolizing heme to iron *(37)*. Shortly thereafter, it was determined that heme oxygenases (HOs) are responsible for the breakdown of heme *(38, 39)*. The enzymatic breakdown of heme by HOs prevents the accumulation of free heme and mitigates its toxic effects *(40)*.

Concurrently with ferrous iron, heme (predominately with ferric iron) degradation by HOs results in the production of carbon monoxide (CO) and biliverdin (BV) (Figure 1) *(38, 39)*. HOs additionally require oxygen and electrons from NADPH to perform their enzymatic reaction, as follows:

$$Heme^{3+} + 3O_2 + \frac{9}{2}NADPH + \frac{7}{2}H^+ \longrightarrow Fe^{2+} + CO + BR + \frac{9}{2}NADP^+ + 3H_2O \quad (41)$$

Subsequently, BV is converted into bilirubin (BR) by biliverdin reductase (BVR). Both BV and BR have potent antioxidant properties and help protect cells from oxidative damage *(42, 43)*. Additionally, BVR has a cytoprotective role by controlling the redox cycle between BR and BV *(44)*. At physiological concentrations, CO acts as a regulatory molecule and has anti-inflammatory and anti-apoptotic effects *(45, 46)*. Additionally, iron is stored in ferritin and sequestered from participating in redox reactions. These effects result in protection for the cell. However, each of these products can have detrimental effects in excess. In newborn infants, excess bilirubin causes hyperbilirubinemia which results in cell toxicity, excess CO inhibits cytochrome c oxidase leading to ROS production and mitochondrial dysfunction, and excess iron generates ROS and can lead to the biologically distinct iron-dependent cell death mechanism named ferroptosis *(47-49)*. Nonetheless, heme degradation products have distinct and essential functions within the cell.

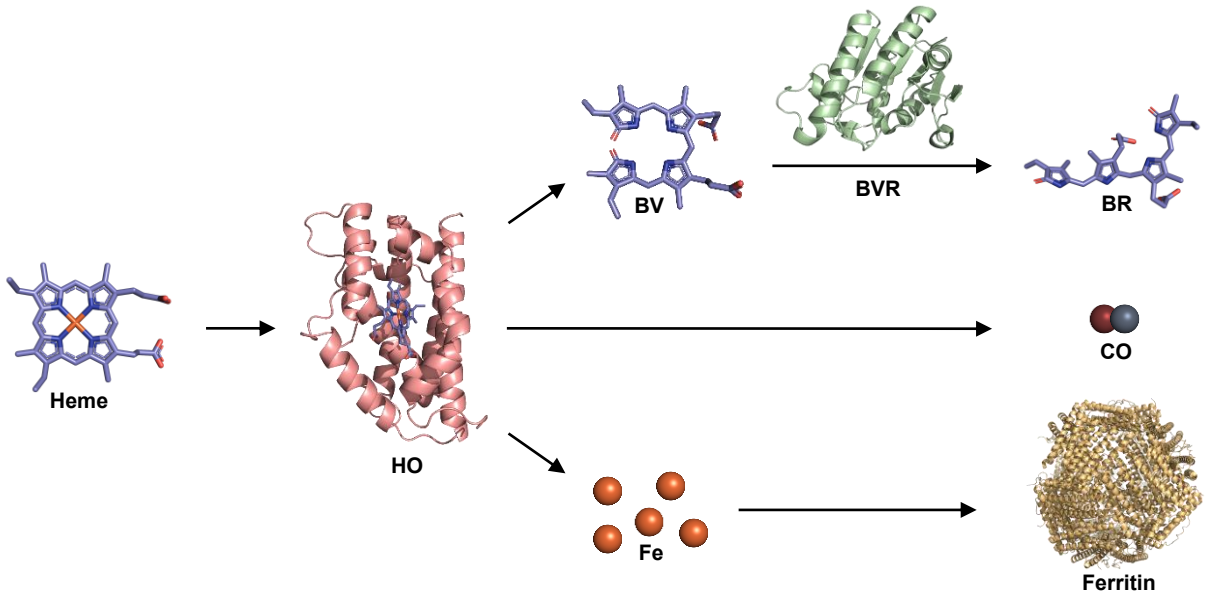

Figure 1. Heme degradation by heme oxygenases. Heme is degraded by heme oxygenase (HO) to produce biliverdin (BV), carbon monoxide (CO), and iron. BV is reduced by biliverdin reductase (BVR) to produce bilirubin (BR). Iron is stored in ferritin. BR (PDB ID: 2VUE); BV (PDB ID: 1BVD); BVR (PDB ID: 1HE4); Ferritin (PDB ID: 4V6B); Heme (PDB ID: 1N3U); HO (PDB ID: 1NI6). Visualized with PyMOL.

There are two heme oxygenase isoforms, HO-1 and HO-2, discovered in the 1980s *(50)*. HO-1 (32kDa) and HO-2 (36kDa) are encoded by *HMOX1* and *HMOX2* genes, respectively, and expressed in most tissues. HO-2 is constitutively expressed while HO-1 is inducible through many stimuli, notably elevated levels of heme and oxidative stress *(51, 52)*. They share 55% sequence identity within the α helical core and high structural homology in the heme binding pocket *(53)*. Within the heme binding pocket is a conserved histidine residue (His25 for HO-1 and His45 for HO-2) critical for coordinating the iron atom of heme and necessary for catalysis *(54, 55)*. For HO-1, the distal Asp140 residue is necessary for catalysis through the coordination of a water molecule needed for maintaining the hydrogen bonding network *(56)*. The helical domain contributes to the overall structural stability of both HOs. Key differences between HO-1 and HO-2 lie in the terminal regions. The C-terminal domains of HO-1 and HO-2 share little sequence homology and, while HO-2 has two heme-regulatory motifs which bind heme independently of

the core, HO-1 lacks heme-regulatory motifs *(53)*. Additionally, HO-2 has a 20-amino acid extension to the N-terminal of unknown significance. The transmembrane anchoring domain of HO-1 and HO-2 facilitates association with the ER membrane and promotes self-association *(57)*. Importantly, HO-1 is cytosol-facing and the transmembrane anchoring region is also important for NADPH binding and maximal enzymatic activity *(58, 59)*. HO-1 is often targeted for therapeutic purposes because its induction under stress conditions suggests a potential role in cellular protection and adaptation, while HO-2, being constitutively expressed, is not typically targeted and is widely considered a housekeeping gene.

HO-1 transcription is governed by several transcription factors and signalling pathways. Nuclear factor erythroid 2-related factor 2 (Nrf2) serves as a pivotal transcription factor central to the upregulation of HO-1 in response to oxidative stress and diverse cellular stressors *(60)*. In unstressed conditions, Nrf2 remains sequestered in the cytoplasm by its inhibitor, kelch-like ECH-associated protein 1 (Keap1). Upon exposure to oxidative stress, electrophiles, or other stress signals, Nrf2 dissociates from Keap1, translocates to the nucleus, binds small Maf protein, and the heterodimer binds to the antioxidant response element and Maf recognition elements located in the HO-1 promoter, promoting transcription *(61, 62)*. Moreover, heme prevents the transcription repressor Bach1, which associates with Maf to form a heterodimer, from binding to Maf recognition elements, rendering Bach1 unable to hinder HO-1 transcription *(63)*. Similarly, hypoxia-inducible factor 1 (HIF-1) responds to low oxygen levels by stabilizing and translocating to the nucleus, binding to hypoxia response elements in the HO-1 promoter, and subsequently upregulating HO-1 expression to aid cellular adaptation to hypoxic environments *(64)*. Furthermore, nuclear factor kappa B (NF-κB), a transcription factor involved in inflammation, promotes HO-1 transcription by binding to specific regulatory sequences in its promoter,

contributing to inflammation resolution *(65, 66)*. Additional transcription factors, including activator protein 1, and signaling pathways, including AKT, MAPK, and STAT3 play roles in regulating HO-1 expression in response to diverse stimuli *(67)*. Collectively, these transcriptional regulators and signaling pathways contribute to the response of HO-1 to various cellular stresses, highlighting its multifaceted cytoprotective functions.

Aside from ER localization, HO-1 is localized to other compartments within the cell. HO-1 has caveolae, mitochondrial, and nuclear localization *(68-70)*. Truncation of the N-terminal of HO-1 leads to increased translocation to the mitochondria where it has been shown to induce mitochondrial dysfunction and increase ROS production *(71)*. Proteolytic cleavage of the C-terminal transmembrane anchoring domain leads to HO-1 (28kDa) translocation to the nucleus *(70)*. A splice variant of HO-1 (14kDa) produced through exon 3 skipping has cytoplasmic localization with distinct roles in cell proliferation and telomere maintenance *(72)*. Notably, non-catalytic HO-1 mutants protect cells against oxidative stress, highlighting a role for non-canonical functions of HO-1 *(73)*. Indeed, within the nucleus, catalytic and non-catalytic HO-1 regulate transcription factor DNA binding *(70)*. Moreover, catalytic and non-catalytic HO-1 are capable of self-regulation during oxidative stress through a positive feedback loop *(74)*. These findings suggest diverse roles for both catalytic and non-catalytic HO-1 depending on localization and protein size.

Within the nucleus are G-quadruplexes (G4s), a non-canonical DNA secondary structure formed by G-tetrads, planar arrangements of four guanine bases that stack on top of each other. G4s are present in over 40% of gene promoter regions and enriched in telomeric regions where they influence chromatin architecture, gene accessibility, and genetic stability *(75-77)*. G4s act as an obstacle in DNA replication by blocking helicase function *(78)*. Furthermore, G4 stabilization

leads to DNA damage by inducing DNA damage and impairing DNA damage repair *(79, 80)*. Heme is a natural ligand for G4s, tightly binding within the G-tetrad core and promoting G4 formation *(81)*. HO-1 has been shown to be implicated in controlling labile nuclear heme levels, have a function in DNA damage response, and have a possible role in resolving G4s *(82)*. Combined, these findings suggest a role for HO-1 in mitigating G4-related DNA damage.

Heme oxygenase-1 in disease and cancer

Dysregulation of HO-1 has been implicated in various diseases and cancers, reflecting its dual role as both a cytoprotective enzyme and a mediator of certain pathological processes. The aberrant expression and activity of HO-1 contributes to the pathogenesis of several conditions including inflammatory, cardiovascular, metabolic, and nervous system diseases as well as cancers *(83-87)*. Induction of HO-1 has proven beneficial for favorable outcomes in these diseases, whereas inhibition of HO-1 is desirable for favorable outcomes in cancers *(83-87)*. Consequently, efforts have been made to develop effective inducers and inhibitors of HO-1.

In many diseases, HO-1 expression contributes to positive outcomes. Thus, there has been work done to create effective HO-1 inducers. Natural products are a major category of compounds and several have shown effectiveness in inducing HO-1 expression, including quercetin, curcumin, and thymoquinone *(88)*. Cobalt protoporphyrin, a heme analog, has been shown to be an inducer of HO-1 *(89)*. Additionally, HO-1 has been induced through induction of its transcription factors, Nrf2 and HIF-1 *(90)*. CO, a product of heme degradation by HO-1, has been used as proxy for HO-1 induction. It has been proposed that CO is responsible for the increased survival imparted by HO-1 *(91, 92)*. Subsequently, a class of compounds was identified with the ability to release CO, aptly named carbon monoxide-releasing molecules (CORMs) *(93)*. At their core, CORMs are metal carbonyls, which are coordination complexes formed by transition metals and carbon

monoxide ligands. Individual CORMs have been designed to release their COs under various settings, such as transiently, through the action of phosphatases and esterases, photochemically, thermally, upon pH change, and by oxidation *(94)*. Moreover, the therapeutic potential of CORMs has been examined in settings such as inflammation, cardiovascular disease, and cancer *(95, 96)*. However, the use of CORMs as CO surrogates has recently been questioned as it has been found that CO release from CORMs may be unreliable and effects of CORMs may be CO-independent *(97)*. Moreover, there are multiple limitations, such as toxicity, reactivity towards proteins, and inaccurate measurements of CO release, contributing to their limited therapeutic application *(98)*.

In cancers, HO-1 overexpression has been linked to cancer progression and resistance to therapy in multiple tumour types, including ovarian and NSCLC *(87, 99, 100)*. Moreover, overexpression of HO-1 leads to increased invasiveness and metastasis in ovarian cancers and NSCLC *(101, 102)*. HO-1 also has a role in modulating the tumor microenvironment, primarily accredited to CO acting as a signaling molecule *(87)*. Consequently, research on HO-1 inhibitors is an active area of investigation. While HO-1 has cytoprotective functions in response to stress, its overexpression can contribute to disease progression. Therefore, inhibiting HO-1 activity is being explored as a strategy to intervene in such disease processes.

The first class of HO-1 inhibitors is metalloporphyrins. Metalloporphyrins are structural analogs of heme with differing coordinated metals. Zinc protoporphyrin (ZnPP) is naturally produced in trace amounts during heme biosynthesis and is used as a substitute by the cell during iron deficiency *(103)*. Early on, ZnPP was discovered to be a selective competitive HO inhibitor *(104)*. In addition, ZnPP has been used in many studies for its selective HO-1 inhibition *(105-107)*. However, researchers later noted that their initial study examined a limited number of biological parameters and that ZnPP has other unintended effects, such as altered glutathione metabolism

(108). Independent of HO-1, ZnPP has been shown to inhibit cyclin D1 expression and suppress cancer cell viability specifically through the Wnt/β-cantenin pathway *(109, 110)*. Moreover, ZnPP has been shown to upregulate HO-1 through increasing promotor binding and through the stress response pathway *(111, 112)*. Due to the analogous structures of metalloporphyrins to heme, they could be used as substitutes for other hemoproteins. Supporting this idea, ZnPP has been shown to interact with other heme-containing enzymes, such as nitric oxide synthase *(113)*. Finally, selectivity for HO-1 over HO-2 is not obtained for tin, chromium, or zinc protoporphyrins *(114)*. These shortcomings have amounted to the limited utility of metalloporphyrins as HO-1 inhibitors.

The second class of HO-1 inhibitors are small molecule inhibitors. A series of imidazole-based compounds have been created and optimized based on a lead compound of azalanstat showing preferential inhibition for either HO-1 or HO-2 *(115-120)*. More recently, an acetamide-based HO-1 inhibitor was developed similarly based on the lead compound of azalanstat *(121)*. These are all non-competitive inhibitors that have the shared function of interacting with the coordinated heme iron within the heme binding pocket. One competitive HO-1 inhibitor has been synthesized, a quinoline-based imidazole derivative *(122)*. Of these inhibitors, only one of the imidazole-based compounds is purchasable, through MedChemExpress (HY-111798A). However, despite the high inhibitory activity of these inhibitors in *in vitro* reconstitution assays, there is limited cytotoxicity in cancer cells, demonstrated by half maximal inhibitory concentrations (IC_{50}) between 10 and 50 μM for MCF-7 breast cancer cells *(120, 122, 123)*. Nonetheless, available inhibitors were used to create a quantitative structure–activity relationship model for ligand-based virtual screening of United States Food and Drug Administration (FDA) approved drugs, natural products, and for novel compounds, resulting in potentially interesting candidates *(118, 124, 125)*.

While small molecule inhibitors remain the most selective and potent HO-1 inhibitors developed so far, their therapeutic efficacy continues to be insufficient.

HO-1 inhibitors represent a promising avenue for therapeutic intervention in diseases where HO-1 overexpression plays a role. Continued research is needed to refine the specificity and efficacy of these inhibitors and to better understand the complex interplay of HO-1 in different pathological contexts. Moreover, as most current options are non-competitive and rely on inhibiting the heme degradation by HO-1 after binding, there is a need for competitive inhibitors to block the ability of HO-1 to coordinate heme effectively.

AIMS

Previous work has illuminated heme metabolism as a vulnerable pathway in SMARCA4-deficient cancers. We hypothesize that targeting HO-1 will induce synthetic lethality in SMARCA4-deficient cancers. To test this hypothesis, this study has two aims:

1. Validate HO-1 as a synthetic lethal target in SMARCA4-deficient cancers while elucidating mechanistic insights for HO-1 dependency.
2. Identify potential therapeutics to exploit this HO-1 dependency through structure-based virtual screening.

METHODS

Tissue cell culture

BIN-67, OVCAR4, SCCOHT-1, SKOV3, H1299, H1703, H1703B11, H358, and HCC827 cells were cultured in RPMI media with 6% fetal bovine serum, 1% penicillin/streptomycin antibiotics, and 2mM L-glutamine. HEK-293 cells were cultured in DMEM media with 6% fetal bovine serum, 1% penicillin/streptomycin antibiotics, and 2 mM L-glutamine. All cell lines were grown at 37˚C and 5% CO2 levels. Cells were refreshed or passaged every 3-4 days. When cells reached a ~80% confluency, BIN-67 and H358 cells were passaged at a ratio of 1:3, OVCAR4, SCCOHT-1, H1703, H1703B11, HCC827, and HEK-293 cells at a ratio of 1:5, and SKOV3 and H1299 cells were passaged at a ratio of 1:10. When passaging, cells were first washed with 1X phosphate buffer saline (PBS) solution and trypsinized at 37˚C for 1-2 minutes using 0.05% trypsin-EDTA (1X) solution. Cells were kept in culture for approximately 8 weeks.

Compounds and antibodies

Dihydroergotoxin mesylate (HY-B0799), Rolapitant (HY-14751), Lomitapide (HY-14667), Venetoclax (HY-15531), Zafirlukast (HY-17492), Galloylpaeoniflorin (HY-N5048), Solanosine (HY-N0070), Tricarbonyldichlororuthenium(II) dimer (CORM-2) (HY-W033577), Bilirubin (HY-N0323), Biliverdin hydrochloride (HY-135005), Bilirubin Conjugate disodium (HY-129834), and Heme Oxygenase-1-IN-I hydrochloride (HY-111798A) were purchased from MedChemExpress. The inactive form of CORM-2 (iCORM-2) was prepared by leaving the compound for 18 hours at 37℃ in a 5% carbon dioxide humidified atmosphere to release CO *(126)*.

The antibodies used for Western blot analysis include cleaved PARP (5625S; Cell Signalling), HO-1 (43966S; Cell Signalling), β-actin (sc-47778; Santa Cruz), α-tubulin (T6199;

Sigma-Aldrich), Lamin B1 (ab16048; Abcam), and Tim23 (11123-1-AP; Proteintech). Antibody against β-actin was used at 1:5000 dilution, and all others were used at 1:1000 dilution. All antibodies were diluted in 2% BSA.

The antibodies, fluorochromes, stain used for immunofluorescence microscopy include HO-1 (43966S; Cell Signalling), Tom20 (sc-17764; Santa Cruz), Alexa Fluor 488 conjugated anti-rabbit (A-21206; Invitrogen), Alexa Fluor 647 conjugated anti-mouse (A-31571; Invitrogen), and DAPI (4′,6-diamidino-2-phenylindole) (1:5000 in mounting media). Antibodies against HO-1 and Tom20 were used at 1:100 dilution and secondary fluorophore antibodies were used at 1:1000 dilution. All antibodies were diluted in blocking solution (5% donkey serum, 2% BSA, 0.1% Triton X-100, 0.05% Tween in 1X PBS).

Plasmids

shRNA vectors were obtained from the MISSION® lentiviral shRNA libraries (TRC1, 1.5 and 2) (Sigma-Aldrich) offered by the McGill Platform for Cellular Perturbation (MPCP) of the Goodman Cancer Institute and Biochemistry at McGill University. Once picked from bacterial glycerol stocks, bacteria carrying the plasmid of interest were cultured overnight in 5 mL of LB broth and selected for with ampicillin. The plasmid was then isolated using the Plasmid DNA Miniprep Kit by Bio Basic or the Genopure Plasmid Maxi Kit by Roche. DNA concentrations were quantified using a NanoDrop spectrophotometer.

Two shRNAs targeting the *HMOX1* gene were picked with differing vectors:

- shHMOX1 #1 TRCN0000290435: ACAGTTGCTGTAGGGCTTTAT (pLKO.5)

- shHMOX1 #2 TRCN0000045250: ACAGTTGCTGTAGGGCTTTAT (pLKO.1)

One shRNA targeting the *EIF2AK1* gene was picked:

- shEIF2AK1 TRCN0000196737: GTACAATGCTTCGTTGTATTT (pLKO.1)

Virus production and transduction

HEK-293 cells were transfected with a mixture containing the following reagents: 2 ug of isolated DNA (shRNA), 2 ug of packaging plasmid mix, 200 µL of HBS-buffer pH 6.95-7.05, and 10.5 µL of 2.5M $CaCl_2$. Using a 0.45 mm syringe filter unit designed for virus production, the first tap of virus was collected 24 hours post-transfection and the second tap at 36 hours post-transfection. Following, cells were infected with the collected virus and polybrene was added. The remaining virus was snap-frozen in liquid nitrogen and then stored at -80˚C for later use. Lentiviral transduction was performed following the Broad Institute Genetic Perturbation Platform's protocol found at http://www.broadinstitute.org/rnai/public/resources/protocols. 30 hours post-infection, infected cells were selected for using the selection marker 2 µg/ml puromycin for 2-3 days.

Cell viability assays

Cells were seeded into 96-well plates at a low density (200-5000 cells per well). Background control wells were included for each cell line. CellTiter-Blue viability assays (Promega) were performed 6-8 days post-seeding. For drug treatment experiments, cells were refreshed 24 hours post-seeding with drug, and CellTiter-Blue viability assays (Promega) were performed 3 days post-seeding. For analysis, cell viability indexes were normalized from background fluorescence and then standardized to negative controls (for shRNA: pLKO, for drug: untreated).

Colony formation assays

Cells were seeded into 6-well plates at a low density (2-50x10^4 cells per well). 24 hours post-seeding, media was refreshed with or without drug with subsequent refreshes every 3-4 days. The experiment was terminated once the negative control (for shRNA: pLKO, for drug: untreated or drug carrier) had reached approximately 80% confluency. At end points, assays were fixed with 4% formaldehyde, stained with 0.1% w/v crystal violet, and scanned.

Immunofluorescence (IF) microscopy

Cells were seeded into 12-well plates on glass coverslips at a medium density (2.5-6x10^4 cells per well). 48 hours post-seeding, cells were fixed (4% formaldehyde), permeabilized (0.1% Triton-100, 0.1M glycine in 1X PBS), and blocked (5% donkey serum, 2% BSA, 0.1% Triton X-100, 0.05% Tween in 1X PBS). Cells were simultaneously incubated in a mixture of two primary antibodies raised in different species (i.e., mouse and rabbit) overnight at 4°C. Cells were then simultaneously incubated in a mixture of two secondary antibodies raised in the same species (i.e. donkey) for 1 hour at room temperature. Coverslips were mounted with Fluorescence Mounting Medium (Dako) and stored in the dark at 4°C until imaging. Samples were imaged using the 63x oil objective of the LSM 710 Confocal Microscope (ZEISS) in the McGill University Advanced BioImaging Facility (ABIF). Images were processed using ZEN (ZEISS) and Fiji (ImageJ).

Protein lysate preparation and Western blot analysis

Cells were seeded into 6-well plates at a high density (3-6x10^5 cells per well). 24 hours post-seeding, cells were washed with PBS, lysed with protein loading buffer, heated at 90˚C for 4 minutes, and analyzed with Novex® NuPAGE® Gel Electrophoresis Systems (Invitrogen) and with Amersham ECL Western blotting detection reagent. The following protocols were utilized:

http://www.bio-rad.com/webroot/web/pdf/lsr/literature/10007296D.pdf and

http://www.bio-rad.com/webroot/web/pdf/lsr/literature/M1703930.pdf.

Subcellular fractionation

For nuclei isolation, cells in 1 ml of ice-cold PBS were collected using cell scrapers from 10 cm dishes on ice, grown to approximately 80% confluency, and washed twice with ice-cold PBS. Cells were pelleted, resuspended with hypotonic buffer (20 mM Tris pH 7.4, 10 mM KCl, 2 mM $MgCl_2$, 1 mM EGTA, 0.5 mM DTT, 0.5 mM PMSF) and incubated for 3 minutes. Pellet was resuspended with 0.3% NP40-PBS and incubated for 3 minutes (taking an aliquot of supernatant as whole lysate fraction), pelleted again (taking an aliquot of supernatant as cytoplasmic fraction), resuspended/washed with isotonic buffer (20 mM Tris pH 7.4, 150 mM KCl, 2 mM $MgCl_2$, 1 mM EGTA, 0.5 mM DTT, 0.5 mM PMSF), and incubated 5 minutes. After centrifugation, the insoluble fraction was resuspended with 0.3% NP40-PBS for 3 minutes and pelleted (nuclear fraction) with supernatant discarded. The cytoplasmic fraction was centrifuged at high speed to pellet debris. A 3:1 ratio of sample to 4x protein lysis buffer was added to the whole and cytoplasmic fractions while the nuclear fraction was resuspended in 1x protein lysis buffer. The whole lysate and nuclear fractions were sonicated for 30 seconds, and all samples were heated at 90˚C for 4 minutes.

Intracellular ROS determination

Intracellular ROS levels were obtained following the DCFDA / H2DCFDA - Cellular ROS Assay Kit (ab113851) from Abcam. Briefly, cells were plated at a medium density in a 96-well plate ($2.5x10^5$ cells per well). Cells were incubated with dichlorodihydrofluorescein diacetate (DCFDA) for 45 minutes, resulting in the production of the highly fluorescent compound DCF through oxidation by ROS. Measurements were taken at Ex/Em = 485/535 nm.

Hemin levels determination

Hemin levels were obtained following the Hemin Assay Kit (MAK036) from Sigma-Aldrich. Briefly, cells were plated in a 6-well plate at $2x10^6$ cells per well. Cells were trypsinized and pelleted in 1.5 ml Eppendorf tubes, washing once with PBS. PBS was removed, cells were resuspended in 4 volumes of cold hemin assay buffer, and centrifuged at a high speed (13 000 x g for 10 minutes at 4˚C) to remove insoluble material. Samples were diluted between 100 and 1000-fold and plated at 50 µl in a 96-well plate. The reaction mix was added into each well, consisting of 3 µl of enzyme mix, 2 µl of hemin substrate, 43 µl of hemin assay buffer, and 2 µl of hemin probe. Hemin standard solution was used to create a standard curve. Reactions were mixed thoroughly and left to incubate. Measurements were taken at 570 nm every hour until absorbance was in the range of 0.7–1.3.

Protein structures

Hemoprotein structures include heme-free HO-1 (PDB ID: 1NI6), heme-bound HO-1 (1N3U), myeloperoxidase (PDB ID: 1CXP), hemoglobin (PDB ID: 1GZP), nitric oxide synthase (PDB ID: 1M9J), hemopexin (PDB ID: 1QJS), cytoglobin (PDB ID: 1UMO), inducible nitric oxide synthase (PDB ID: 2NSI), heme oxygenase-2 (PDB ID: 2QPP), cytochrome b5 oxidoreductase (PDB ID: 3LF5), myoglobin (PDB ID: 3RGK), cytochrome c (PDB ID: 3ZCF), neuroglobin (PDB ID: 4MPM), cytochrome p450 (PDB ID: 5VBU), cytochrome c oxidase (PDB ID: 5Z62), catalase (PDB ID: 7VD9), and eukaryotic translation initiation factor 2-alpha kinase 1 obtained through the AlphaFold Protein Structure Database.

Virtual screening

The HO-1 structure used as a docking receptor for the virtual screens was determined by x-ray crystallography and absent of heme binding (PDB ID: 1NI6). AutoDock Vina was used as the search engine due to its efficiency, compatibility with iron-containing ligands, and ease of use *(127, 128)*. Protein structures were prepared by deleting water, adding polar hydrogens, and adding Kollman charges. Ligands were obtained from ZINC15 for drugs preapproved by major regulators (N=5470), Collection of Open Natural Products (COCONUT) for natural products (N=99,626), and *REAL* Database for widescale screening (N=49,792,235) *(129-131)*. ZINC15 and COCONUT ligands were hydrated and converted to 3D structures before use. Proteins, ZINC15 ligands, and COCONUT ligands were converted to PDBQT files using AutoDockTools *(132)*. The grid was centered on the iron-coordinating amino acid's terminal R group atom. The VirtualFlow platform was used for the initial docking of *REAL* Database ligands, using QuickVina2 and Smina as engines and heme-bound HO-1 as the docking receptor (PDB ID: 1N3U) *(133)*. The grid box size was optimized based on ligand size for ZINC15 ligands, COCONUT ligands, and top hits from the VirtualFlow screening (N=804) *(134)*. AutoDock Vina was utilized to conduct docking experiments for ZINC15 ligands, COCONUT ligands, and top hits from the VirtualFlow screening. For these ligands, the global search exhaustiveness value was set to 8 with the energy range set to 4kcal/mol. Scripts were ran through local processing and batch processing on supercomputer clusters overseen by the Digital Research Alliance of Canada. Structures were visualized using PyMOL. Chemical structures were drawn using ChemDraw.

Statistical analysis

Statistical significance was calculated by two-way ANOVA, Tukey's multiple comparison test, and two-tailed t-test. The test used and number of independent experiments performed (n) are indicated

in the figure caption. All Western blots and images shown are representatives of independent experiments. Prism 8 software was used to generate graphs and statistical analyses. Error bars represent mean ± standard deviation. *$p < 0.05$, **$p < 0.01$, ***$p < 0.001$, and ****$p < 0.0001$.

RESULTS

Validating HO-1 as a synthetic lethal target in SMARCA4-deficient cancers

Our lab has previously determined heme metabolism to be a vulnerable pathway in SMARCA4-deficient cancers (unpublished). As HO-1 has an integral role in heme metabolism, we interrogated its role as a potential target that is dependent by these cancer cells. To study HO-1 in SMARCA4-deficient cancers we used the following cancer cell lines: SMARCA4-deficient ovarian (BIN-67, SCCOHT-1) and lung (H1299, H1703) cancer lines plus SMARCA4-proficient ovarian (OVCAR4, SKOV3) and lung (H1437, HCC827) cancer cells. Of note, BIN-67, SCCOHT-1, and H1703 are additionally SMARCA2-deficient while H1299 and SMARCA4-proficient cancer cells are SMARCA2-proficient. We also utilized H1703B11, which is a stable clone of H1703 with SMARCA4 restoration. Using two independent shRNAs targeting *HMOX-1*, we did selective HO-1 knockdown using lentiviral transduction. *HMOX-1* targeting shRNAs were effective in knocking down HO-1 knockdown in all cell lines (Figure 2A). Of note was the high basal expression of HO-1 in SMARCA4-deficient cancers, particularly that in SCCOHT-1 and H1703, suggesting that these cancer cells may depend on elevated HO-1. In short-term cell viability assays, HO-1 knockdown was effective in selectively killing SMARCA4-deficient ovarian cell lines compared to SMARCA4-wild type ovarian cancer cells (Figure 2B). HO-1 knockdown was also effective in selectively killing SMARCA4-deficient NSCLC cell lines (Figure 2C). In the isogenic cell pair, we observed increased cancer-cell killing of HO-1 knockdown for SMARCA4-deficient H1703 compared to SMARCA4-restored H1703B11 (Figure 2D).

Long-term colony formation assays showed that HO-1 knockdown led to significantly reduced cell proliferation in SMARCA4-deficient ovarian cancer cells (Figure 2E). Inhibition of proliferation was similarly seen in SMARCA4-deficient lung cancer cells (Figure 2F). The

isogenic cell pair (H1703B11 vs H1703) showed more moderate difference in terms of inhibition of proliferation upon HO-1 knockdown (Figure 2G). These results established HO-1 knockdown to be an effective target for selectively killing SMARCA4-deficient cancers.

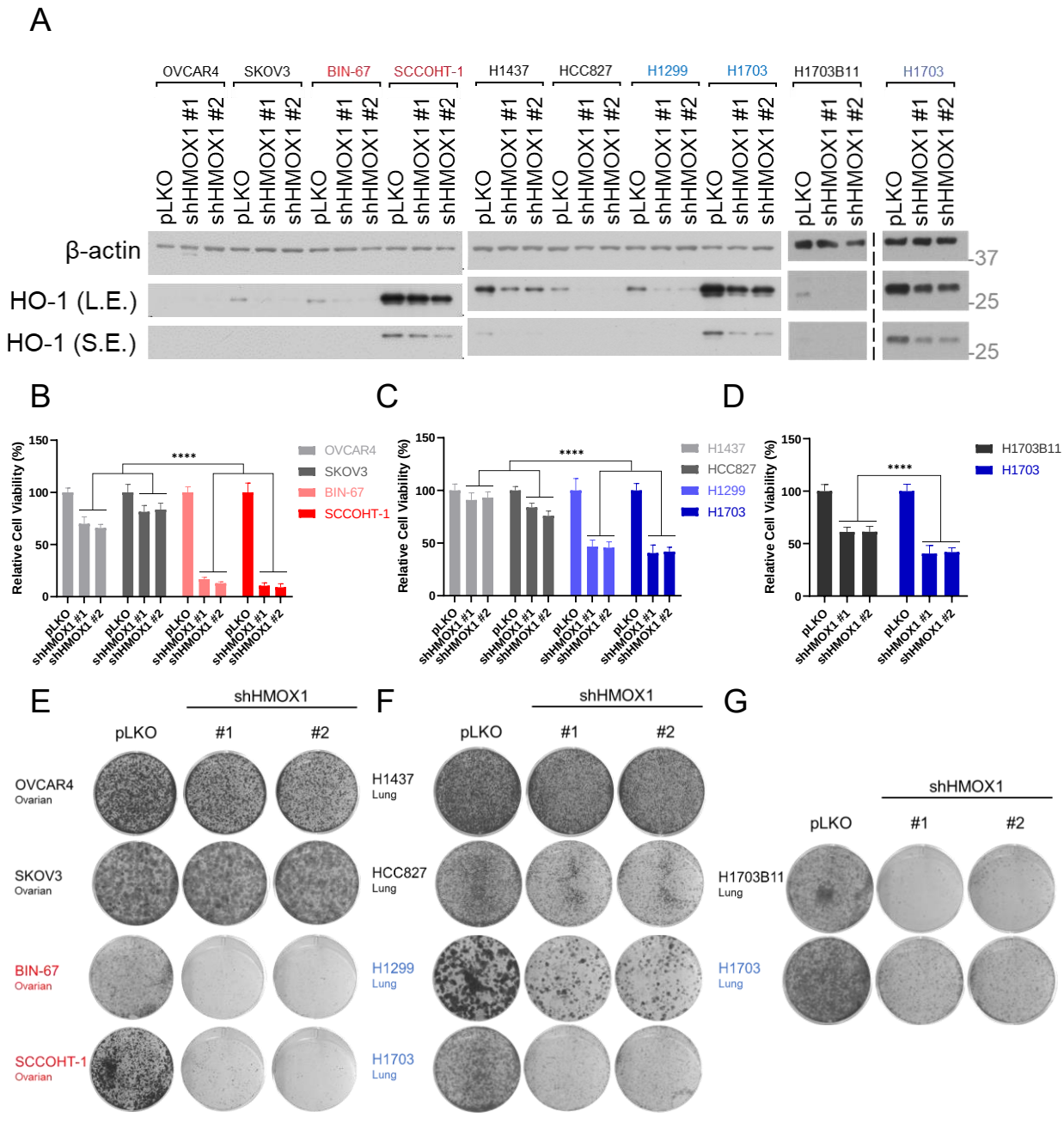

Figure 2. HO-1 is a synthetic lethal target for SMARCA4-deficient ovarian and lung cancers. (A) Validation of HO-1 knockdown by Western blot analysis. Representative of n=3 independent experiments. Cell lines are labelled as follows: greys for SMARCA4-proficient, reds for ovarian SMARCA4-deficient, and blues for SMARCA4-deficient lung cancer cells. (B-D) Short-term cell viability assay following HO-

1 knockdown by shRNA in (B) ovarian cancer cells, (C) lung cancer cells, and (D) a SMARCA4-isogenic cell pair. OVCAR4, n=3; SKOV3, n=3; BIN-67, n=3; SCCOHT-1, n=3; H1437, n=2; HCC827, n=2; H1299, n=2, H1703, n=4; H1703B11, n=3 independent experiments. Cells were plated at a medium density and stained with CellTiter-Blue once pLKO reached confluency after 6-8 days post-seeding. pLKO was used as a negative knockdown control and for normalization. Two-way ANOVA. (E-G) Long-term colony formation assay for HO-1 knockdown in (E) ovarian cancer cells, (F) lung cancer cells, and (G) a SMARCA4 isogenic cell pair. Representative of n=3 independent experiments. Cells were seeded at a low density and cultured for approximately 2 weeks before being fixed and stained horizontally. ****$p < 0.0001$. Error bars, mean ± SD.

HO-1 is mostly localized to the cytoplasm enriched with endoplasmic reticulum in SMARCA-deficient cancer cells

HO-1 has varying functions depending on cellular localization *(68-70)*. Localization knowledge is important for obtaining insight into its mechanism of function and for designing potential therapeutics. For example, HO-1 has roles in signaling which are independent of its catalytic function *(70)*. HO-1 has a cleaved variant created under stress conditions and it expected to be localized in the nucleus *(70)*. Thus, to determine the relevancy of this truncated variant in SMARCA4-deficient cancers, we completed subcellular fractionations in SMARCA4-deficient cell lines. The Western blot results demonstrated that full-length HO-1 is present in the whole cell and cytoplasmic fractions but not in the nuclear fractions. In addition, the truncated variant was present in the whole cell and cytoplasmic fraction of only SCCOHT-1 cells, while absent in the nuclear fraction (Figure 3A).

Aside from protein analysis, spatial analysis through immunofluorescence (IF) microscopy can give insight into localization. IF of HO-1 in ovarian (SKOV3, SCCOHT-1) and lung (H1703) cell lines demonstrated that HO-1 is expressed ubiquitously throughout the cell, with little to no localization to the nucleus (Figure 3C-E). Additionally, there was a substantial overlap between HO-1 and the mitochondria (TOM20), although this may be an artifact of generalized cytoplasmic localization. Nonetheless, it appeared that HO-1 aggregated to form distinct puncta, aligning with previous HO-1 IF imaging *(71, 135, 136)*. Relative expression of HO-1 in SMARCA4-proficient

SKOV3 appeared much lower than in SMARCA4-deficient cancers, as to be expected from Western blot analysis. Taken together, our results suggest that HO-1 is mainly present in the ER enriched cytoplasm of our cells regardless of SMARCA4 status, albeit with more abundance in SMARCA4-deficient cells.

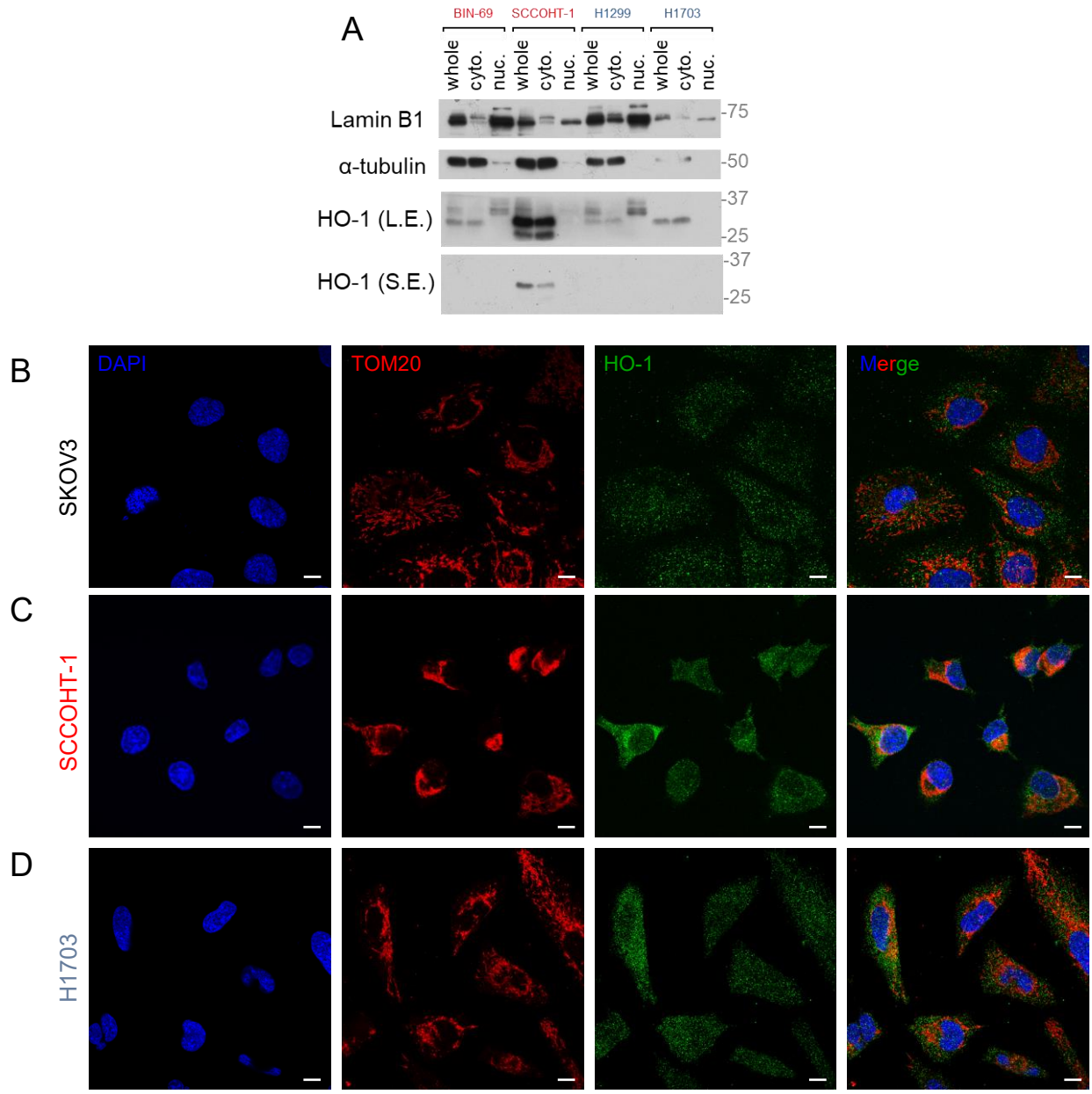

Figure 3. HO-1 is expressed in the cytosol enriched with endoplasmic reticulum. (A) HO-1 is present in cytoplasmic fractions and reduced in nuclear fractions of SMARCA4-deficient cancer cells by Western blot analysis. Representative of n=3 independent experiments. Cell lines are labelled as follows: black for

SMARCA4-proficient, reds for ovarian SMARCA4-deficient, and blues for SMARCA4-deficient lung cancers. (B-D) Immunofluorescence (IF) microscopy images for (B) SKOV3, (C) SCCOHT-1, and (D) H1703. n=1. HO-1 is expressed ubiquitously throughout the cells with higher expression in SMARCA4-deficient cancer cells. Samples were prepared as per IF protocol and imaged using the LSM 710 Confocal Microscope (63x oil objective) (ZEISS) and processed with ZEN and Fiji software. DAPI – blue, TOM20 (mitochondria marker) – red, HO-1– green. Scale bar, 10µm.

Knockdown of HO-1 causes cell death in SMARCA4-deficient cancers in part through heme-induced DNA damage

Given cytoplasmic localization of HO-1, it seemed likely that the catalytic action of HO-1 may be integral to its essential functionality in SMARCA4-deficient cancers. To elucidate the mechanism, we first examined intracellular ROS content after HO-1 knockdown. Heme itself can be a producer of ROS through oxidation of the coordinated iron atom *(31)*. Additionally, assuming catalytic function, knocking down HO-1 would lead to a decrease in metabolites CO and bilirubin which are known to be cytoprotective partially through reducing ROS *(42, 46)*. Interestingly, following HO-1 knockdown there was little to no change in ROS levels in SMARCA4-proficient ovarian cancer cells, while there was a significant decrease in ROS levels in SMARCA4-deficient ovarian cancer cells (also deficient in SMARCA2) (Figure 4A). Among lung cancer cells, H1703 (deficient in both SMARCA4 and SMARCA2) exhibited a similar reduction in ROS levels although this was not observed in the case of H1299 (SMARCA4-deficient but SMARCA2 proficient) or SMARCA4-proficient cells (Figure 4B). Therefore, HO-1 or iron produced from heme degradation may contribute a larger role to ROS production than heme itself.

We then sought to measure the intracellular heme concentration with HO-1 knockdown. Upon HO-1 knockdown, there was an increase in heme concentrations, only in the SMARCA4-deficient ovarian cancer (Figure 4C). Eukaryotic initiation factor 2-alpha kinase 1 (EIF2AK1) was used as a positive control, a heme-binding protein that increases intracellular heme levels upon knockdown as determined by previous work in our lab (unpublished). Within a HO-1 low

environment, heme itself has been shown to be toxic through two avenues, heme-induced ER stress and DNA damage *(35, 36)*. Probing for the DNA damage marker γH2AX and apoptosis marker cleaved PARP revealed increased levels following HO-1 knockdown in SMARCA4-deficient ovarian cancers (Figure 4D). Similarly, this trend was also observed in SMARCA4-deficient lung cancers (Figure 4E). These results suggest that the elevated heme induced by HO-1 knockdown may cause DNA damage, which in part contributes to the selective killing in SMARCA4-deficient cancer cells.

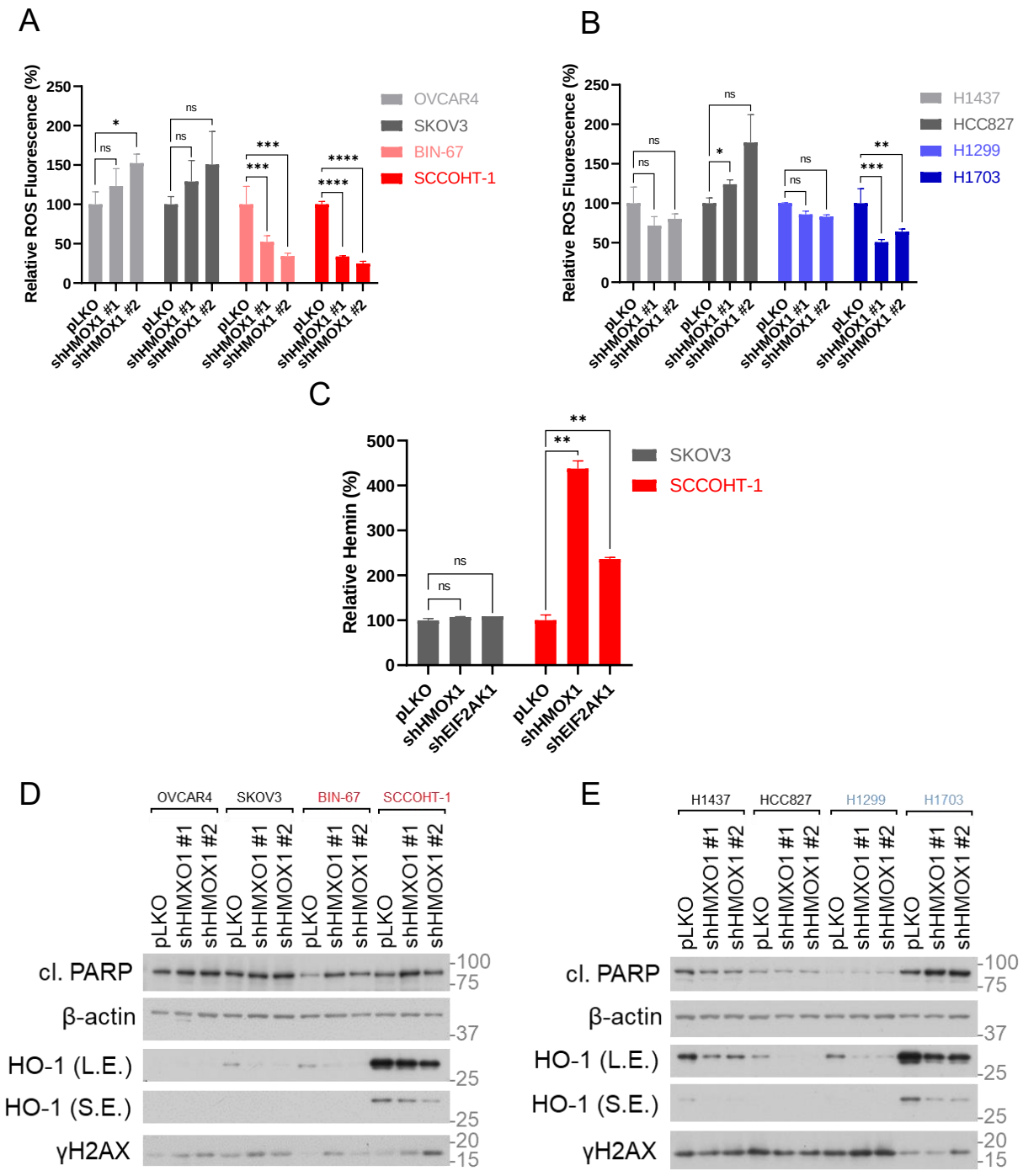

Figure 4. HO-1 knockdown causes cell death by heme toxicity. (A-B) Intracellular reactive oxygen species (ROS) content after HO-1 KD by shRNA as measured by DCF fluorescence after incubation with DCFDA for 45 minutes for (A) ovarian and (B) lung cancer cells. OVCAR4, n=4; SKOV3, n=4; BIN-67, n=3; SCCOHT-1, n=3; H1437, n=1; HCC827, n=2; H1703, n=2; H1703, n=2 independent experiments. Two-tailed t-test. Cell lines are labelled as follows: black for SMARCA4-proficient, reds for ovarian SMARCA4-deficient, and blues for SMARCA4-deficient lung cancers. pLKO is used as a negative knockdown control and for normalization. (C) Hemin levels content after HO-1 knockdown or EIF2AK1 knockdown by shRNA in ovarian cancer cells as measured by fluorescence following the Hemin Assay

Kit (Sigma-Aldrich). n=1. Two-tailed t-test. (E-F) Increase in DNA damage and apoptosis as probed by γH2AX and cleaved PARP, respectively, in SMARCA4-deficient (E) ovarian and (F) lung cancer cells by Western blot analysis. Representative of n=2 independent experiments. *p < 0.05, **p < 0.01, ***p < 0.001, and ****p < 0.0001. Error bars, mean ± SD.

Therapeutic strategies targeting HO-1 for selectively killing SMARCA4-deficient cancer cells

Since results pointed toward the importance of HO-1 catalytic activity, we sought to target SMARCA4-deficient cancers through the metabolites of HO-1. Elevated levels of HO-1 metabolites, CO and BR, have toxic properties *(47, 48)*. We hypothesized that elevated HO-1 levels would lead to an increase in HO-1 metabolites which could lead to exploitable imbalances. CORM-2 is a rubidium-containing molecule that has passively released COs conjugated to the metal, while inactivated CORM-2 (iCORM-2) is prepared by pre-releasing CO. Treating ovarian cancer cells with CORM-2 led to selectivity towards SMARCA4-deficient cells, particularly that of SCCOHT-1 (Figure 5A). Similarly, lung cancer cells treated with CORM-2 led to selectivity towards SMARCA4-deficient cells, particularly that of H1299 (Figure 5B). Treating cells with BR resulted in minimal selectivity in ovarian and lung cancers (Figure 5C and 5D). Overall, CO, or at least CORM-2, can be used to selectively kill SMARCA4-deficient cancer cells.

A more direct method for modulating HO-1 catalytic activity is through inhibitors, of which two main classes exist: non-competitive inhibitors that block protoporphyrin ring cleavage through coordination with the iron atom in the HO-1 binding pocket and metal protoporphyrins which are heme analogs. Treatment with a non-competitive heme oxygenase-1 inhibitor (HO1i) resulted in reduced cell viability in SMARCA4-deficient ovarian cancers at the highest doses tested (Figure 5E). Treatment with HO1i resulted in reduced cell viability in SMARCA4-deficient lung cancers as well as H1437 to a similar degree as H1299 (Figure 5F). The sensitivity of H1437 could be due to the relatively high expression of HO-1 in this cell line (Figure 2G). Between the SMARCA4-

isogenic cell pair, there was selectivity of HO1i for H1703 over H1703B11 (Figure 5G). Zinc protoporphyrin (ZnPP) competitively binds to the active site of HO-1 and cannot be degraded. Treatment with ZnPP resulted in similar trends in the reduction of cell viabilities for SMARCA4-deficient ovarian cancers, lung cancers, and between the SMARCA4-isogenic cell pair (Figure 5H-J).

While some selectivity is seen using HO-1 inhibitors, these inhibitors may not have optimal functionality for the desired outcome of heme toxicity. The non-competitive inhibitor is selective for HO-1, but it allows HO-1 to continue to coordinate heme, while the zinc protoporphyrin is a competitive inhibitor, but it lacks selectivity towards HO-1. Since ZnPP is a structural analog to heme, it can interact with other proteins that use heme as a prosthetic group *(113)*. These results suggest that the heme coordinating activity and not necessarily the heme degradation by HO-1 may be essential for its protective mechanisms. Thus, an effective inhibitor to induce heme toxicity as by HO-1 knockdown would be a HO-1 selective competitive inhibitor.

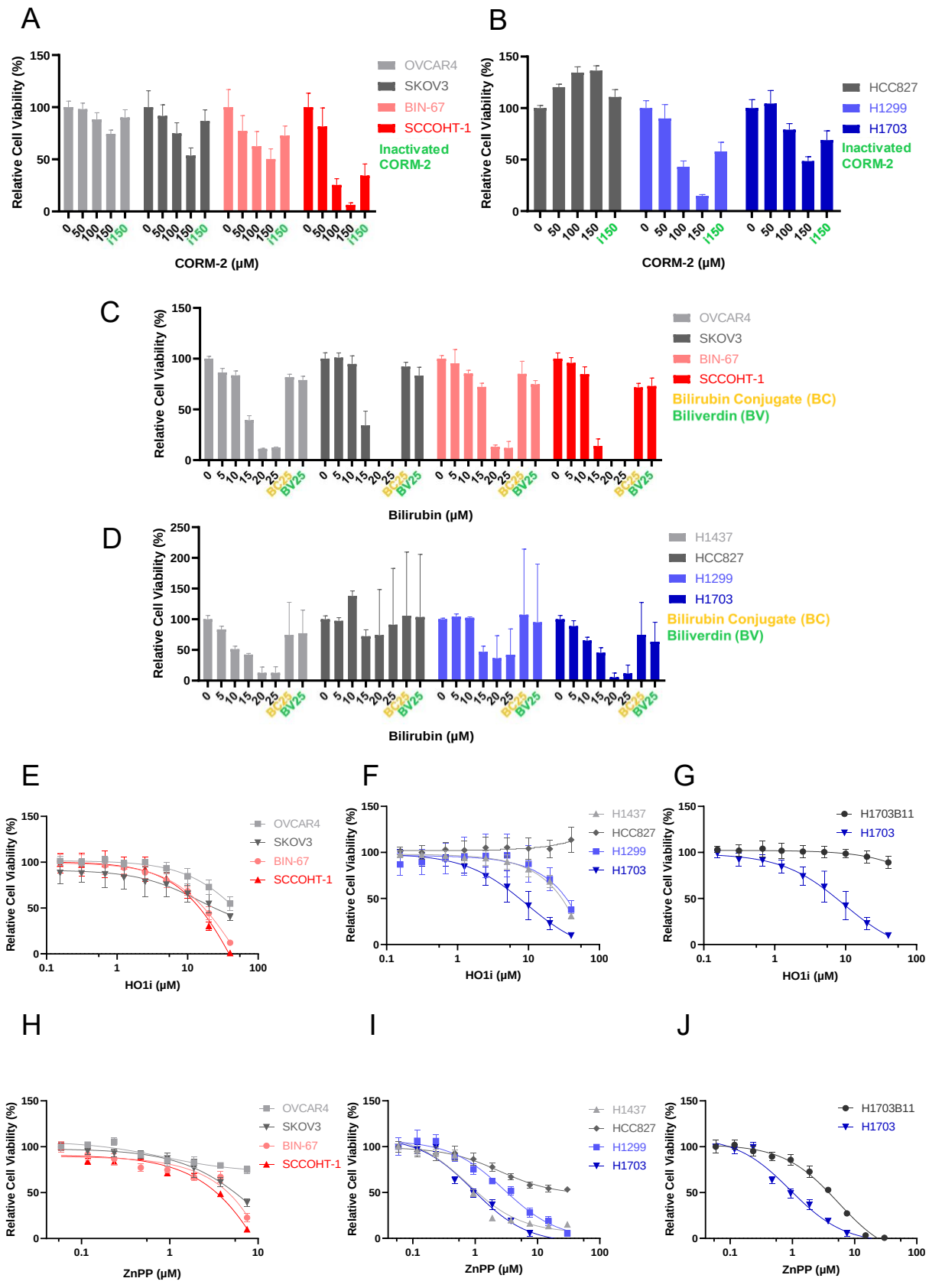
A
Relative Cell Viability (%)
CORM-2 (μM)
OVCAR4
SKOV3
BIN-67
SCCOHT-1
Inactivated CORM-2
B
HCC827
H1299
H1703
C
Bilirubin (μM)
Bilirubin Conjugate (BC)
Biliverdin (BV)
D
H1437
E
HO1i (μM)
F
G
H1703B11
H
ZnPP (μM)
I
J

Figure 5. CORM-2 and HO-1 inhibitors cause cell death in SMARCA4-deficient lung and ovarian cancers. (A-B) Cell viability assay following 3-day CORM-2 treatment for (A) ovarian and (B) lung cancers. Cell lines are labelled as follows: greys for SMARCA4-proficient, reds for ovarian SMARCA4-deficient, and blues for SMARCA4-deficient lung cancers. OVCAR4, n=4, SKOV3, n=4; BIN-67, n=2; SCCOHT-1, n=3; HCC827, n=1; H1299, n=1; H1703, n=1 independent experiments. Cells were treated 24 hours post-seeding and stained with CellTiter-Blue at endpoint. Inactivated CORM-2 (iCORM-2; labelled in green) was prepared by pre-releasing CO and used as a control for the metal's effect. (C-D) Cell viability assay following 3-day bilirubin treatment for (C) ovarian and (D) lung cancers. n=1. Bilirubin conjugate (BC; gold) and biliverdin (BV; green) were used as negative controls. (E-G) Cell viability assay following 3-day HO-1 inhibitor (HO1i) treatment in (A) ovarian cancers, (B) lung cancers, and (C) a SMARCA4-isogenic cell pair. OVCAR4, n=2, SKOV3, n=3; BIN-67, n=3; SCCOHT-1, n=3; HCC827, n=3; H1299, n=3; H1703, n=2; H1703B11, n=3 independent experiments. (H-J) Cell viability assay following 7-day zinc protoporphyrin (ZnPP) treatment in (A) ovarian cancers, (B) lung cancers, and (C) a SMARCA4-isogenic cell pair. n=1. All panels normalized to untreated condition.

Virtual screening to identify existing drugs to be repurposed as HO-1 inhibitors

As there are no known potent selective competitive HO-1 inhibitors, we set out to utilize *in silico* screening to identify novel HO-1 blockers. Virtual screening functions as a predictive tool to reduce the initial set of compounds tested *in vitro (137)*. Previous studies for HO-1 inhibitor discovery focused on ligand-based methods using azalanstat, an imidazole-based compound, as a lead structure. We wanted to focus on structure-based molecular docking between the ligand and the heme binding pocket of HO-1 to ensure competitiveness.

HO-1 (PDB ID: 1NI6) is a homodimer that has a distinct binding pocket for heme where the coordinated iron of heme interacts with His25, which is essential for catalytic activity (Figure 6A). Molecular docking, using AutoDock Vina as the search engine, estimates the binding of heme to HO-1 to be -10.4kcal/mol, averaged between chains A and B (Figure 6A). The first set of virtual screens used drugs approved by major jurisdictions worldwide obtained from the ZINC15 database, intending to repurpose an accessible drug. Results of compounds docked (N=5740) had a range of binding affinities of ligands for HO-1 chain A and chain B, with those of interest near or surpassing the binding affinity of heme to HO-1 (-10.4kcal/mol) (Figure 6B).

From the screens, the top hits chosen to follow for testing were lomitapide, rolapitant, venetoclax, zafirlukast, and dihydroergotoxine mesylate (Supplemental Table 1). These drugs were

chosen due to their favourable predicted binding affinities and availability. Lomitapide, rolapitant, venetoclax, and zafirlukast had minimal selectivity towards SMARCA4-deficient ovarian cancers (Figure 6C-F). Dihydroergotoxine had the best selectivity for SCCOHT-1 of the drugs in ovarian cancers (Figure 6G). The long-term colony formation assay mirrored these results of some selectivity towards dihydroergotoxine for SMARCA4-deficient ovarian cancers (Figure 6H). In lung cancers, dihydroergotoxine had the best selectivity for SMARCA4-deficient H1703 and H1299 cells although there was greatly reduced cell viability in SMARCA4-proficient H1437 as well (Figure 6I), which could be explained by elevated HO-1 expression in H1437 (Figure 2G). In the SMARCA4-isogenic cell pair, dihydroergotoxine had a large selectivity against SMARCA4-deficient H1703 (Figure 6J). These results demonstrated that structure-based virtual screening could be an effective tool for finding novel HO-1 inhibitors.

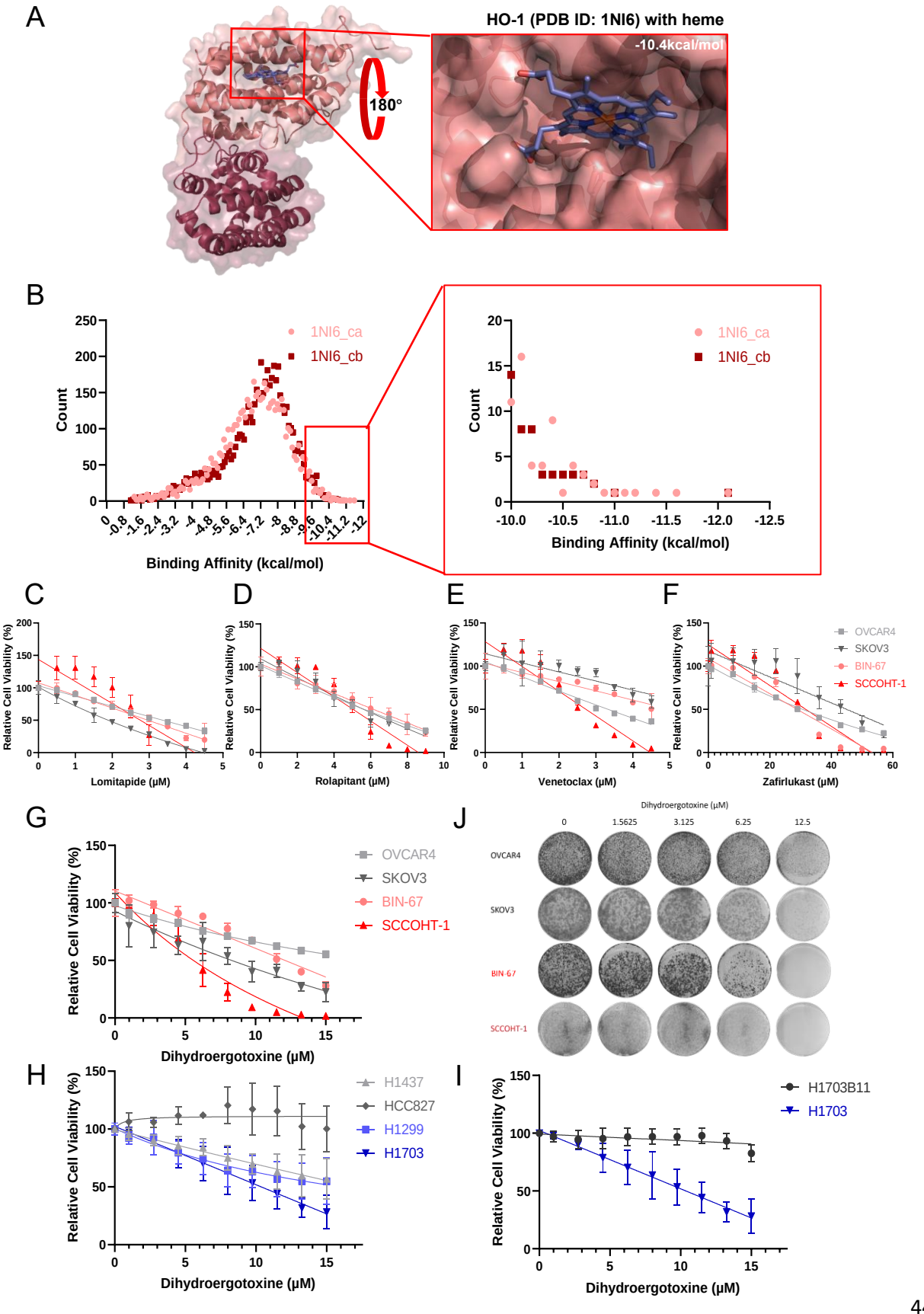
A
HO-1 (PDB ID: 1NI6) with heme
-10.4kcal/mol
180°
B
1NI6_ca
1NI6_cb
Count
Binding Affinity (kcal/mol)
C
Relative Cell Viability (%)
Lomitapide (μM)
D
Rolapitant (μM)
E
Venetoclax (μM)
F
Zafirlukast (μM)
OVCAR4
SKOV3
BIN-67
SCCOHT-1
G
Dihydroergotoxine (μM)
J
Dihydroergotoxine (μM)
0
1.5625
3.125
6.25
12.5
H
H1437
HCC827
H1299
H1703
I
H1703B11
H1703

Figure 6. Dihydroergotoxine from virtual screening of common drugs showed some selectivity for SMARCA4-deficient ovarian and lung cancers. (A) HO-1 homodimer (PDB ID: 1NI6) with heme in the binding pocket. Average binding affinity: -10.4kcal/mol. Colouring: chain A (ca) – salmon; chain B (cb) – raspberry; heme – blue. Visualized with PyMOL. (B) HO-1 homodimer chain A and B virtual screen binding affinity overview for drugs from the ZINC15 database (N=5470). Points represent count per decimal. (C-F) Cell viability assay following 3-day (C) lomitapide (-11kcal/mol), (D) rolapitant (-10.35kcal/mol), (E) venetoclax (-11.1kcal/mol), and (F) zafirlukast (-9.95kcal/mol) treatments for ovarian cancers. n=1. Binding affinities are given as the average between chains A and B. Cell lines are labelled as follows: greys for SMARCA4-proficient, reds for ovarian SMARCA4-deficient, and blues for SMARCA4-deficient lung cancers. Cells were treated 24 hours post-seeding and stained with CellTiter-Blue at endpoint. (G-I) Cell viability assay following 3-day dihydroergotoxin (-10.7kcal/mol) treatment for (G) ovarian cancers, (H) lung cancers, and (I) SMARCA4-isogenic cell pair. OVCAR4, n=1; SKOV3, n=2; BIN-67, n=1; SCCOHT-1, n=1; H1299, n=2; HCC827, n=2; H1299, n=2; H1703, n=2; H1703B11, n=2 independent experiments. (J) Colony formation assay following dihydroergotoxin treatment in ovarian cancers. Representative of n=2 independent experiments. Cells were seeded at a low density and cultured for approximately 2 weeks before being fixed and stained horizontally.

Identifying and testing natural products as HO-1 inhibitors

Next, we sought to expand the scope of the search to include a greater number of potential inhibitors. For this, we tested an array of natural products from the COCONUT database since natural produces can make good drug candidates due to their diverse and complex chemical structures *(130)*. Results of compounds docked (N=99,626) had a range of binding affinities of ligands for HO-1 chain A and chain B, with those of interest near or surpassing the binding affinity of heme to HO-1 (-10.4kcal/mol) (Figure 6A).

From the screens, top hits chosen to follow for testing were galloylpaeoniflorin and solasonine (Supplemental Table 2). These compounds were chosen because of their favorable predicted binding affinities and availability. Galloylpaeoniflorin showed no selectivity for SMARCA4-deficient cancers (Figure 7B-D). Solasonine showed poor SMARCA4-deficient selectivity for ovarian cancers, some selectivity for lung cancers, and selectivity between the SMARCA4-isogenic cell pair (Figure 7E-G). Validation of other hits would be necessary to form conclusions on the efficacy of the present virtual screens.

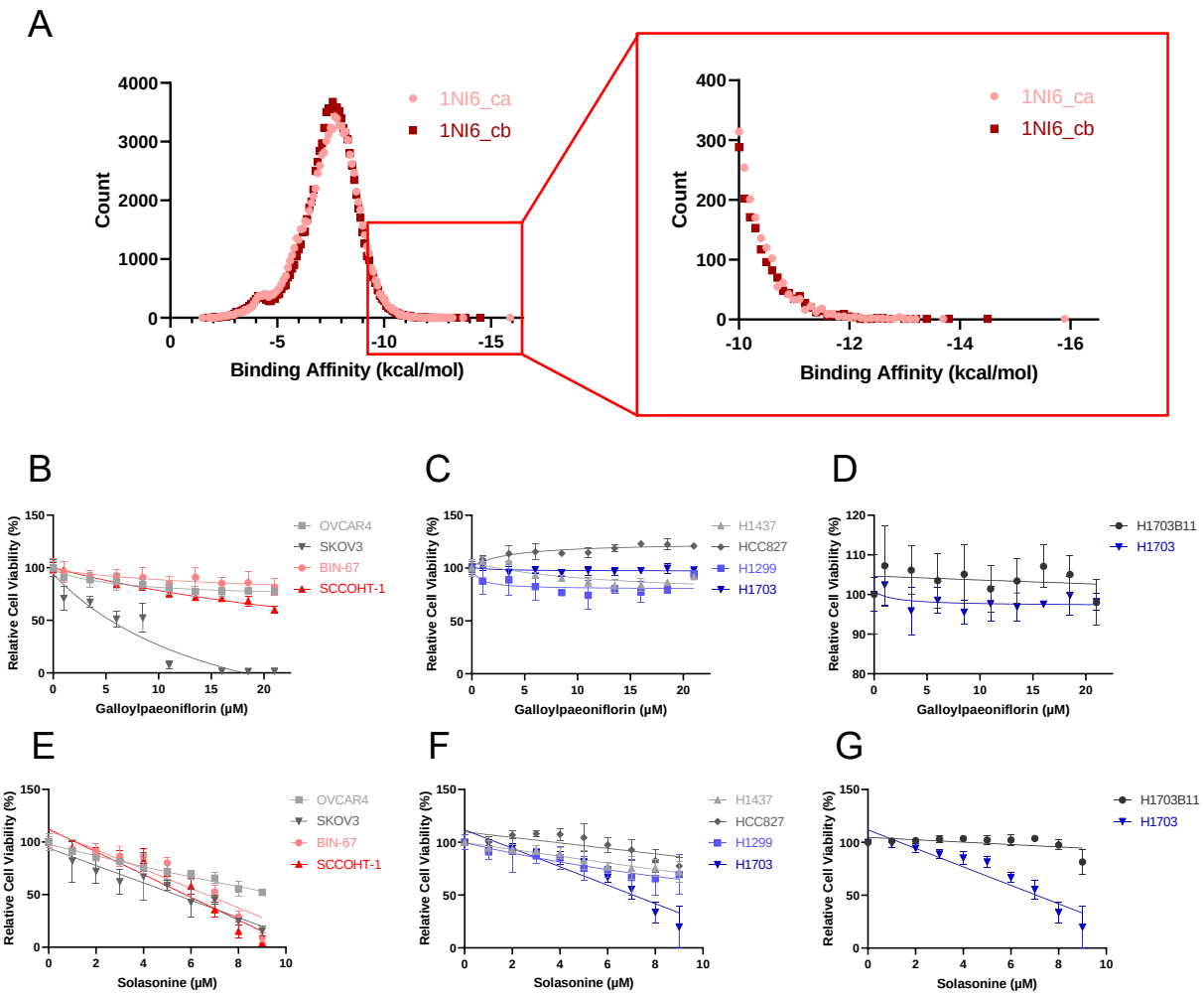

Figure 7. Natural products virtual screening led to products with limited selectivity for SMARCA4-deficient ovarian and lung cancers. (A) HO-1 homodimer chain A and B (PDB ID: 1NI6) virtual screen binding affinity overview for natural products from the Collection of Open Natural Products (COCONUT) database (N=99 626). Colouring: chain A (ca) – salmon; chain B (cb) – raspberry. Points represent count per decimal. (B-D) Cell viability assay following 3-day galloylpaeoniflorin (-9.7kcal/mol) treatment for (B) ovarian cancers, (C) lung cancers, and (D) SMARCA4-isogenic cell pair. n=1. Binding affinities are given as the average between chains A and B. Cell lines are labelled as follows: greys for SMARCA4-proficient, reds for ovarian SMARCA4-deficient, and blues for SMARCA4-deficient lung cancers. Cells were treated 24 hours post-seeding and stained with CellTiter-Blue at endpoint. (E-F) Cell viability assay following 3-day solasonine (-12.7kcal/mol) treatment for (E) ovarian cancers, (F) lung cancers, and (G) SMARCA4-isogenic cell pair. OVCAR4, n=1; SKOV3, n=1; BIN-67, n=1; SCCOHT-1, n=2; H1299, n=1; HCC827, n=2; H1299, n=1; H1703, n=2; H1703B11, n=1 independent experiments. Binding affinities are given as the average between chains A and B.

Uncovering novel synthetic compounds as HO-1 inhibitors

For the final virtual screens, we sought to test a large array of novel compounds. Following the VirtualFlow platform, ligands from the Enamine *REAL* Database, which consists of novel compounds that exist in real space and can be synthesized and ordered, were tested *(131)*. The portion of the database that is available with the VirtualFlow platform consists of over 1.4 billion compounds, thus, a subset of the database was considered consisting of approximately 102 million compounds. Of the 102 million compounds, almost 50 million compounds were tested, running on 4000 jobs across 4 superclusters for a month.

The VirtualFlow screen resulted in a large distribution of binding affinities. During ligand preparation, some ligands were improperly converted, resulting in "broken" ligands. Thus, the top 10,000 ligands were filtered for having a real structure (N=804) and rescreened following the previously established workflow using AutoDock Vina (Figure 8A). Of these 804 potential drug candidates, the top 120 were carried forward for further analysis, with a few hits having better average binding affinity than heme to HO-1 (-10.4kcal/mol), indicating the top candidates for competitiveness (Figure 8B).

Another important consideration for choosing the candidates is their selectivity towards HO-1. To determine this, we first determined the binding affinity of heme to various hemoproteins (Figure 8C). From here, the binding affinity of each candidate was determined in each hemoprotein. The difference in binding affinities of the candidate from the hemoproteins to HO-1 was obtained, and results were normalized to heme's binding affinity to the individual hemoprotein and summed (Figure 8D). Several candidates had an overall preference for HO-1 as compared to hemoproteins, as indicated by a larger normalized sum value, indicating the top candidates for selectivity.

Between the top twenty competitive and selective candidates, seven candidates overlapped (Supplemental Table 3). Two of the twenty top dual competitive and selective ranked within the top four for both categories (Compounds 71 and 106). These two candidates, along with the other top three from each category, were visualized for individual binding to each hemoprotein (Figure 8E). Of note, Compound 71 had preferential binding towards HO-1 over 11/15 of hemoproteins. Cytochrome c had poor binding affinity for heme resulting in visually exaggerated preference of candidates over HO-1. Each candidate has the general structures of two ends of bulky aromatic rings connected by a linker that contains a ketone group. Within the binding pocket, each compound can utilize the ketone group for an electrostatic interaction or an aromatic ring for π-π stacking with the catalytic His25 of HO-1, moreover, the ends can be utilized for anchoring within the binding pocket (Figure 8F). Virtual screening uncovered potential novel competitive and selective drug candidates for HO-1 to be explored further.

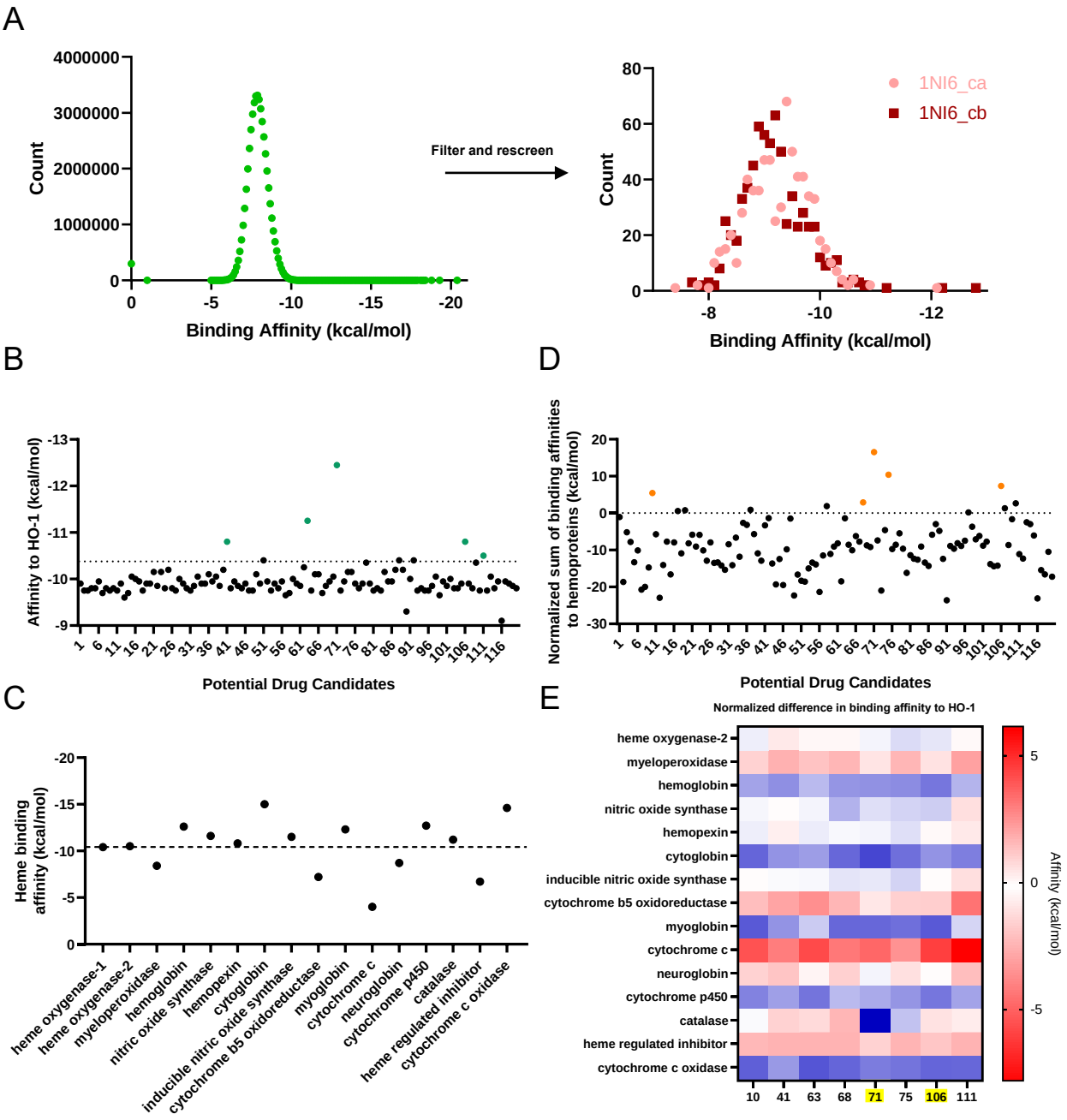
A
Count
Binding Affinity (kcal/mol)
Filter and rescreen
1NI6_ca
1NI6_cb
B
Affinity to HO-1 (kcal/mol)
Potential Drug Candidates
C
Heme binding affinity (kcal/mol)
heme oxygenase-1
heme oxygenase-2
myeloperoxidase
hemoglobin
nitric oxide synthase
hemopexin
cytoglobin
inducible nitric oxide synthase
cytochrome b5 oxidoreductase
myoglobin
cytochrome c
neuroglobin
cytochrome p450
catalase
heme regulated inhibitor
cytochrome c oxidase
D
Normalized sum of binding affinities to hemoproteins (kcal/mol)
Potential Drug Candidates
E
Normalized difference in binding affinity to HO-1
Affinity (kcal/mol)
F
Example

Figure 8. Virtual screening of novel compounds led to three top candidates for HO-1 heme binding competition and selectivity. (A) Left: Virtual screen binding affinity overview following the VirtualFlow platform for novel compounds in HO-1 chain A (PDB ID: 1N3U) (N=49 792 235). Right: HO-1 homodimer chain A and B (PDB ID: 1NI6) virtual screen binding affinity overview for filtered top hits from VirtualFlow (N=804). Colouring: chain A (ca) – salmon; chain B (cb) – raspberry. Points represent count per decimal. (B) Binding affinities of the top 120 potential drug candidates to HO-1. Binding affinities are given as the average between chain A and B. Dotted line represents heme binding affinity to HO-1 (-10.4kcal/mol). Top 5 competitive candidates are highlighted in blue. (C) Binding affinities of heme to hemoproteins. Heme regulated inhibitor and cytochrome c oxidase are given as the average between two heme binding sites. (D) Normalized sum of binding affinities of the top 120 potential drug candidates to hemoproteins. Each hemoprotein is normalized for its heme binding affinity and normalized to the binding affinity of heme to HO-1. Top 5 selective candidates are highlighted in orange. (E) Heatmap of top competitive and selective potential drug candidates normalized difference in binding affinity between hemoprotein and HO-1. Positive affinity (blue) indicates preference towards HO-1 and negative affinity (red) indicated preference towards hemoprotein. Each hemoprotein is normalized for its heme binding affinity. Dual top competitive and selective candidates (Compounds 71 and 106) are highlighted in yellow. (F) Example compound fin HO-1 heme binding pocket. Visualized with PyMOL.

Overall, we propose that HO-1 has an integral role in maintaining intracellular heme levels, and through its perturbation, heme causes apoptosis through double-stranded DNA breaks (Figure 9). Perturbation can come in the form of genetic perturbation (e.g., shRNA), as demonstrated in the present study, or inhibitors, which need to continue to be optimized. Hindering the ability of HO-1 to breakdown or coordinate heme leads to its increased intracellular levels, resulting in DNA damage and ultimately apoptosis. Whether this effect is moderated through heme induced G4 stabilization or another mechanism is yet to be determined.

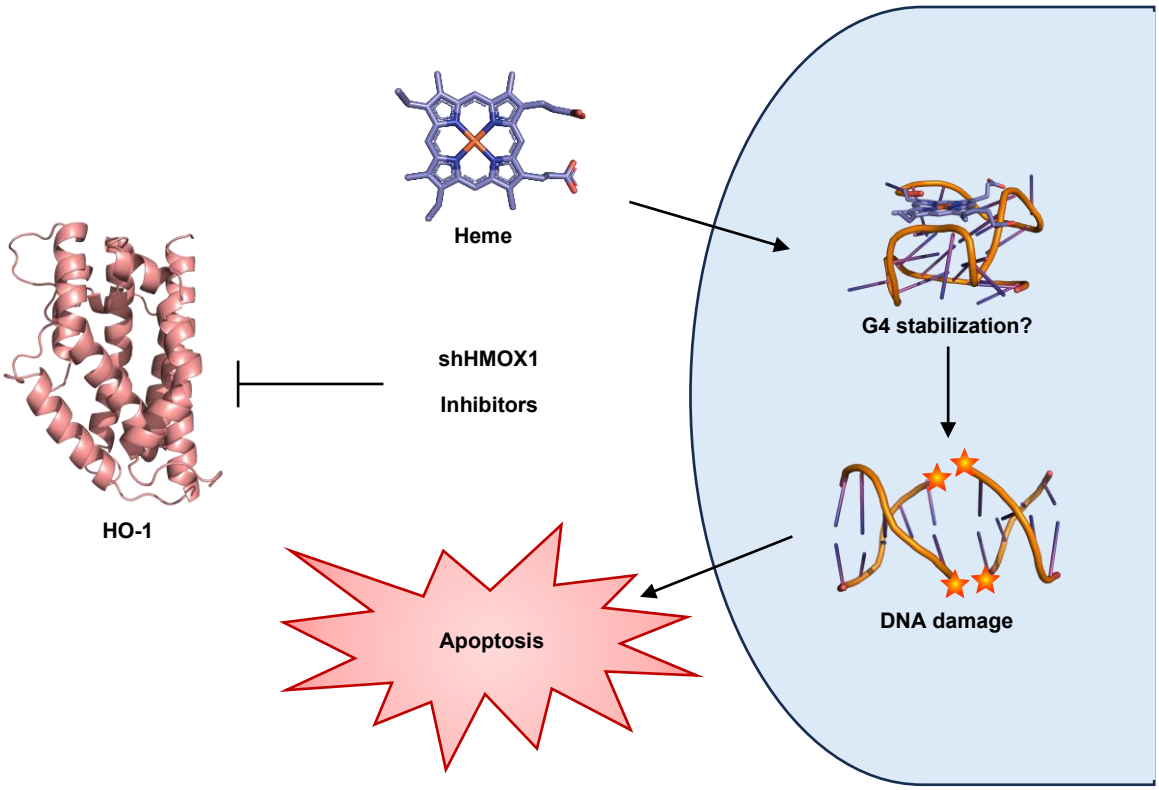

Figure 9. Proposed model for the mechanism behind the synthetic lethal interaction between HO-1 and SMARCA4. SMARCA4-deficient cancers have a synthetic lethal relationship with the heme degrading protein HO-1. HO-1 perturbation leads to increased intracellular heme levels, DNA damage, and ultimately apoptosis. Heme can stabilize G4s, a DNA secondary which tightly binds heme and causes genetic instability and DNA damage. The present link between heme and G4s continues to be elucidated. DNA (PDB ID: 1ZEW); G4: G-quadruplex (PDB ID: 1XAV); Heme (PDB ID: 1N3U); HO-1: Heme oxygenase-1 (PDB ID: 1NI6). Visualized with PyMOL.

DISCUSSION

Treating SMARCA4-deficient cancers, such as SCCOHT (~100%) and NSCLC (~10%), proves challenging due to limited available treatment options and the ineffectiveness of conventional chemotherapy *(22-25)*. This study aimed to validate and characterize HO-1 as a synthetic lethal target in SMARCA4-deficient cancers and identify potential novel inhibitors. Selective knockdown of HO-1 induced synthetic lethality, reduced ROS, and increased DNA damage markers. Therapeutically, CORMs, specifically CORM-2, selectively targeted SMARCA4-deficient cancers. Current HO-1 inhibitors are limited due to selectivity, competitiveness, and potency *(114, 120, 122, 123)*. Virtual screening identified dihydroergotoxin as a promising candidate for HO-1 inhibition. Natural products virtual screening identified solasonine showing limited selectivity. Novel compounds with a central ketone group and end aromatic ring structures were identified by virtual screening as potential competitive and selective HO-1 inhibitors, highlighting the need for further exploration of these candidates.

Our lab previously identified heme metabolism as a vulnerable target in SMARCA4-deficient cancers following a synthetic lethal shRNA screen. In the present study, selective knockdown of HO-1 was shown to cause synthetic lethality in SMARCA4-deficient significantly over SMARCA4-proficient cancers. Cancer cell lines were chosen based on availability. Presumably, similar findings would be applied to other SMARCA4-deficient cancer cells, however, further testing would be needed to validate this claim. Sensitivity towards HO-1 knockdown was greater in SCCOHT compared to SMARCA4-deficient NSCLCs (Figure 2B-F). This could be attributed to the more complex mutation landscape in NSCLC compared to SCCOHT, which has a simple genome. Notably, there is a significant, albeit small, selectivity of HO-1 knockdown in SMARCA4-deficient H1703 as compared to SMARCA4-isogenic control

H1703B11 in short term viability assay, and this selectivity is absent in the colony formation assay (Figure 2D, G). Perhaps the naturally occurred SMARCA4-deficient cancer cells acquire additional adaptations during tumorigenesis, in addition to high HO-1 expression, which is unable to be reversed by SMARCA4 restoration. Additionally, selectivity could be a product of SMARCA4-regulated HO-1 levels as we observed that there is decreased basal HO-1 expression in H1703B11 (Figure 2A). While SMARCA4 does not directly regulate HO-1, SMARCA4 does regulate Nrf2 signaling, the predominate transcription factor of HO-1, with increased HO-1 expression observed in SMARCA4-deficient NSCLCs due to Nrf2 binding the *HMOX1* promoter *(138)*. These findings underscore the therapeutic potential of targeting HO-1 in SMARCA4-deficient cancers, and highlight the intricate interplay of mutation landscapes, cellular adaptations, and SMARCA4 regulation in determining sensitivity to HO-1 knockdown.

HO-1 has a variety of functions based on its localization. Of note are its nuclear and mitochondrial localizations *(70, 71)*. The nuclear form of HO-1 is believed to contribute to transcription factor DNA binding and is C-terminally cleaved to remove its transmembrane domain which anchors it to the ER membrane *(70)*. The cleaved form of HO-1 was observed in SCCOHT-1 by Western blot, however, its localization to the nucleus was not observed via immunofluorescence (Figure 3A-B). The predominant localization for HO-1 was observed to be the cytosol, containing the ER. Looking at the overlap between mitochondrial and HO-1 staining, HO-1 may exist at the mitochondrial ER interface, a notion that is yet to be addressed. Supporting this idea, HO-1 is important for heme degradation which occurs in the mitochondria, and is tightly regulated to protect the cell from hemes harmful effects *(40)*. However, more precise imaging would be needed to form conclusions.

Surprisingly, there was a reduction in ROS with HO-1 knockdown in SMARCA4-deficient cancers (Figure 4A, B). Decreased ROS was unexpected as HO-1 knockdown led to increased heme levels, which is known to increase ROS *(31)*. However, most studies examine ROS production by heme within the context of HO-1 expression. Heme induces HO-1 expression and, through heme degradation, increases labile iron which can participate in Fenton reactions to produce ROS *(32, 51)*. Thus, decreased ROS with HO-1 knockdown could be due to a greater impact of labile iron on ROS production over heme, as there are no compensatory mechanisms for heme degradation, or a product of HO-1 expression. Indeed, it was found that mitochondrial-localized HO-1 contributes to ROS, potentially coinciding with IF results *(71)*. Further supporting the role of HO-1 in ROS production is the non-significant yet downward trend for ROS in SMARCA4-proficient H1437 cells, which also express relatively high basal HO-1 expression.

Therapeutically, CORMs have been developed to introduce CO, a product of heme degradation by HO-1, to biological systems. CORMs have been shown to have utility in inflammation, cardiovascular disease, and cancer *(95, 96)*. However, the mechanism underlying CORMs effects and ability to act as a CO surrogate has been questioned *(97)*. Notably, CORM-2 was not able to compensate for HO-1 knockdown (data not shown). This result is contrary to the report that CO is responsible for the protective effects of HO-1 and that CO can be compensatory for HO-1 loss *(91, 92)*. Moreover, CORM-2 was shown to selectively target SMARCA4-deficient cancer cells, particularly SCCOHT-1 and H1299 (Figure 5A, B). Lethality is likely due at least partially to CO as iCORM-2 had reduced selectivity. The lethal effect of CORM-2 on SMARCA4-deficient cancers was established while the exact role of CO still needs to be determined.

Increased heme levels within the context of HO-1 knockdown have been shown to induce cell death through heme-induced ER stress and DNA damage in endothelial cell cultures and

mouse-derived macrophages, respectively *(35, 36)*. Heme-induced ER stress is attenuated with HO-1 expression or CORM treatment *(35)*. However, in the present study, we observed selective cell death induced by CORM treatment as well as no increase in ER stress markers by Western blot following HO-1 knockdown (not shown). These results suggest that heme-induced ER stress is likely not the cell death mechanism for SMARCA4-deficient cancers. On the other hand, heme can also induce DNA damage *(36)*. In the present study, we observed an increase in DNA damage marker γH2AX and apoptosis marker cleaved PARP following HO-1 knockdown in SMARCA4-deficient cancers (Figure 4D, E). A prevailing theory explaining heme-induced DNA damage is through G4s. Heme has been shown to stabilize G4s and G4s induce DNA damage, ultimately leading to cell death through apoptosis *(79, 81)*. To address the connection between HO-1 and G4s, one method would be γH2AX staining following HO-1 knockdown and IF imaging to determine the presence of foci, often used as a marker for DNA double-stranded breaks *(139)*. In parallel, it would be insightful to determine any changes in G4s due to HO-1 knockdown-induced intracellular heme increase through IF imaging and measuring affected genes. The stabilizing effect of heme on G4s brings into question the importance of the catalytic activity of HO-1 compared to its heme sequestering ability. Both HO-1 catalytic activity and heme sequestering would effectively decrease the amount of intracellular heme available to interact with G4s, leading to less G4 stability and reduced DNA damage. The link between HO-1 and G4s needs to continue to be explored.

Currently available HO-1 inhibitors are limited by either their competitiveness for heme binding or selectivity. The first class, metalloporphyrins, are structural analogs to heme allowing for their interaction with various hemoproteins (non-selective competitive) *(113)*. Meanwhile, the efficacy and effect of ZnPP are in question as its effects have been attributed to HO-1-independent

mechanisms *(109, 110)*. The second class, small molecule inhibitors, have selectivity for HO-1 while mostly maintaining heme binding (selective non-competitive). Furthermore, the small molecule inhibitors are only effective at high concentrations *(120, 122, 123)*. Thus, a selective competitive inhibitor is necessary to inhibit the heme-coordinating activity of HO-1, leading to heme-induced cell death.

To find competitive inhibitors, we performed structure-based virtual screening based on the heme binding pocket of HO-1. Structure-based molecular docking experiments have improved potential of identifying competitive inhibitors due to the search site being the binding pocket, as compared to previously done ligand-based assays from a non-competitive lead compound azalanstat *(118, 124, 125)*. From docking drugs approved by major jurisdictions, many compounds had predicted binding affinities that competed with that of heme to HO-1 (-10.4kcal/mol) (Supplement Table 1). Of note, the top hit, tasosartan, was not chosen for testing as it was withdrawn from FDA review due to safety trials in phase III clinical trials which would lead to future complications. Venetoclax and lomitapide rank among the top five and were deemed suitable candidates, while rolapitant and zafirlukast ranked lower but with favourable safety profile. Dihydroergotoxin is a mixture of three dihydrogenated ergot alkaloids that share a backbone structure. Within the virtual screens, ergot alkaloids ranked highly, with ergoloid, dihydroergotoxine, ergoloid mesylate, ergotamine ranking within the top ten and dihydroergotamine at the eleventh place. Ergot alkaloids also have acceptable safety profiles lending to their increased desirability as a candidate. In terms of selectivity, dihydroergotoxin had the greatest selectivity for SMARCA4-deficient cancers, to a similar degree as the results of HO-1 inhibitors. However, selectivity was not as strong as with HO-1 knockdown, highlighting the need to find more potent and selective inhibitors.

The natural products virtual screens suffered from the issue of compound availability. To test results that had the best chance of being purchasable, we tested a subset of the database which mostly had explicit names for the compounds, narrowing the compounds by three-fourths (N=407,270 to N=99,626). Nevertheless, many of the top hits continued to be unable to be easily sourced (Supplement Table 2). Among the top four ranked candidates, solasonine, was available for purchase and tested, showing limited selectivity. Galloylpaeoniflorin was a top hit from a previous iteration of the virtual screen and in the final set showed poor predicted binding affinity. Galloylpaeoniflorin showed selectivity towards SMARCA4-proficient SKOV3 which is undesirable in the present context but an interesting result to follow up. These products have previously shown potential as cancer therapeutics *(140, 141)*. Moreover, solasonine has been shown to promote ferroptosis by suppressing glutathione peroxidase 4 and glutathione synthase, where glutathione depletion induces HO-1 *(142, 143)*. This implicates solasonine with HO-1, however, no data points to a direct interaction. The remaining top hits provide valuable information on structural motifs and binding modes within the heme binding pocket.

The selection criteria for the novel compounds virtual screens included favourable properties of small molecules, such as good lipophilicity and hydrogen bond number, narrowing the compounds list from 1.46 billion to 102 million. Of the 102 million compounds, about 50 million of them were run due to time and resource constraints. The initial target used for docking was the heme binding pocket of a heme-bound HO-1 structure (PDB ID: 1N3U) with heme removed from the structure file, and subsequent testing in a heme-free HO-1 structure (PDB ID: 1NI6). There were many false positive hits of ligands that were not properly prepared, appearing as “broken” ligands or having an overall structure that is impossible to exist in real space. This is

a known problem with the current database which aims to have enhanced quality checks in future iterations *(144, 145)*.

Hemoprotein binding was a point of consideration for determining selectivity, however, individual hemoprotein essentiality was not considered. For example, a ligand with off-target effects towards cytoglobin may have less toxicity than one towards cytochrome c oxidase due to the nature of these proteins in cellular function. Cytochrome c had a high affinity for most candidates; however, this is an artifact of cytochrome c having a poor heme binding affinity from the molecular docking experiments, dramatically increasing the apparent preference of the candidates due to normalization. The top two candidates for competitiveness and selectivity had the general structure of bulky aromatic rings at two ends connected by a linker that contains a ketone group (Figure 8F). Within the binding pocket, each compound can utilize the ketone group for an electrostatic interaction or an aromatic ring for π-π stacking with the catalytic His25 of HO-1, moreover, the other end can potentially be utilized for anchoring within the binding pocket. The structure of these candidates is comparable to that of the HO1i with the addition of the center ketone group, which could aid in competitiveness, and bulkier ends, which could aid in selectivity. To test competitiveness, intracellular heme could be measured with and without inhibitor treatment, with treatment expected to displace HO-1 coordinated heme or block heme binding, leading to increased intracellular heme levels. Another method to measure competitiveness would be a kinetic assay, where a competitive inhibitor would allow the reaction to reach the maximum velocity of the enzyme whereas a noncompetitive inhibitor would have a reduced maximum velocity.

Translating these findings to the clinical setting would necessitate optimizing an inhibitor. To accomplish this, efforts must focus on demonstrating the inhibitor's competitiveness and

selectivity for HO-1, as outlined previously. Subsequently, there is a need for testing in cell lines, followed by evaluation in an animal model before progressing to a clinical trial. Aside from SMARCA4-deficient cancer cells, a selective competitive HO-1 inhibitor holds promise for potential application in other cancers expressing elevated levels of HO-1, such as breast, colon, and pancreatic cancers *(87)*. However, caution is advised regarding potential off-target effects, particularly considering high expression of HO-1 in tissues responsible for degrading aged blood cells, such as the spleen *(146)*.

The strength of this study comes from the validation of HO-1 knockdown in SMARCA4-deficient cancers, which was previously undescribed. Additionally, this study is the first report of structure-based virtual screening for finding inhibitors for HO-1.

There are some experimental caveats to be considered. The present study assumed that the effects of the drugs at every stage were imparted by HO-1 inhibition while off-target effects are likely present. The docking software of choice had a major impact on the results obtained, and through another software, other results may rank higher due to differences in scoring methods.

Future directions of this project include further validation of cell death mechanism. The first step would be γH2AX staining and G4 measurements through IF imaging and measuring affected genes following HO-1 knockdown, as previously described. Furthermore, it would be useful to determine the role of a catalytically inactive HO-1 mutant (His25Ala). A catalytically inactive mutant capable of rescuing cell death in SMARCA4-deficient cancers from endogenous HO-1 knockdown points towards heme sequestering being the essential mechanism of HO-1. Importantly, catalytically inactive HO-1 has protective mechanisms unrelated to heme *(70)*. Otherwise, if rescue is not observed, catalytic activity is likely essential. Aligning with this direction would be to directly measure HO-1 enzymatic activity within the cells as only HO-1

expression levels were measured. Additionally, testing novel compounds for efficacy in treating SMARCA4-deficient cancers could be beneficial as well as ligand binding assays to show the interaction between effective ligands and HO-1.

Overall, we hope that this study will contribute to the knowledge of additional treatment modalities in SMARACA4-deficient cancers and perhaps in other contexts where selective competitive inhibition of HO-1 is desirable.

CONCLUSIONS

Our study has validated HO-1, a heme-degrading enzyme, as a novel synthetic lethal target in SMARCA4-deficient cancers, SCCOHT and NSCLC. We reveal that HO-1 knockdown leads to increased intracellular heme levels, DNA damage markers, and apoptosis. These results suggest heme-induced DNA damage as a possible mechanism underlying cell death. Moreover, available HO-1 inhibitors are ineffective at selectively killing SMARCA4-deficient cancers. Through structure-based virtual screening, we identified potential inhibitors from three categories: repurposing common drugs, natural products, and novel compounds. Top candidates validated had some degree of selectivity towards SMARCA4-deficient cancers, similar to that seen with available inhibitors. Continued work should fully explore the connection between increased heme levels and apoptosis as well as identify an effective inhibitor to fully exploit HO-1 as a vulnerability in SMARCA4-deficient cancers.

SUPPLEMENTAL TABLES

Supplemental Table 1. Top 20 purchasable hits from common drug virtual screens.

ZINC ID	Compound Name	Affinity (kcal/mol)	Medicinal Use ***(147)***
ZINC000013444037	Tasosartan	-11.4	NA (liver toxicity)
ZINC000003995616	Ergoloid	-11.2	Age-related cognitive impairment
ZINC000150338755	Venetoclax	-11.1	Leukemia
ZINC000027990463	Lomitapide	-11	Familial hypercholesterolemia
ZINC000006716957	Nitotinib	-10.9	Chronic myelogenous leukemia
ZINC000100378061	Naldemedine	-10.7	Opioid-induced constipation
ZINC000014880002	Dihydroergotoxine	-10.7	Age-related cognitive impairment
ZINC000033359785	Ergoloid Mesylate	-10.7	Age-related cognitive impairment
ZINC000052955754	Ergotamine	-10.6	Acute migraine attacks
ZINC000014210642	Edarbi/Azilsartan	-10.5	Hypertension
ZINC000003978005	Dihydroergotamine	-10.5	Acute migraine attacks
ZINC000003816514	Rolapitant	-10.35	Antiemetic
ZINC000008552017	Ginkgolide B	-10.3	TBD
ZINC000068202099	Erismodegib/Sonidegib	-10.2	Basal cell carcinoma
ZINC000008215434	Flavin adenine dinucleotide	-10.2	Vitamin B2 deficiency
ZINC000038139973	Efonidipine	-10.1	Hypertension
ZINC000053073961	Antrafenine	-10.1	Analgesic
ZINC000064033452	Lumacaftor	-10	Cystic fibrosis
ZINC000000896717	Accolate/Zafirlukast	-9.95	Asthma
ZINC000004096846	Rutin	-9.95	TBD

Affinity is given as the average binding affinity of heme to HO-1 chain A and chain B. Medicinal use determined from the DrugBank. NA: Not available; TBD: To be determined.

Supplemental Table 2. Top 20 hits from natural products virtual screens.

COCONUT ID	Compound Name	Affinity (kcal/mol)	Species of Origin
CNP0074077	Langkocycline B2	-14.85	*Streptomyces* sp. Acta 3034
CNP0475873	Bahamaolide A Tetraacetonide 3	-14.1	*Streptomyces* sp. CNQ343
CNP0454925	Bahamaolide A Tetraacetonide 7	-13.1	*Streptomyces* sp. CNQ343
CNP0252414	Solasonine	-12.7	*Solanum* sp.
CNP0425705	Sanguidimerine	-12.5	*Sanguinaria canadensis*
CNP0415934	Chelidimerine	-12.35	*Chelidonium majus*
CNP0287417	Glycobismine G	-12.25	*Glycosmis citrifolia*
CNP0328740	Clivimine	-12.1	*Clivia miniata*
CNP0351491	Sansanmycin L	-11.9	*Streptomyces* sp. SS
CNP0217217	Sulfadixiamycin B	-11.85	*Streptomyces* sp. HKI0576
CNP0350880	Naseseazine C	-11.75	*Streptomyces* sp. USC-636
CNP0336731	Complanadine B	-11.75	*L. obscurum*
CNP0452454	Plantaricin GZ1-27	-11.7	*Lactobacillus plantarum* GZ1–27
CNP0099867	9-Hydroxycrisamicin A	-11.65	*Micvomonospom* sp. SA246
CNP0092687	Scequinadoline D	-11.6	*Scedosporium apiospermum* F41-1
CNP0182771	Panganensine R	-11.5	*Strychnos panganensis*
CNP0429038	Platensimycin D1	-11.45	*Streptomyces platensis* SB12029
CNP0304662	Moromycin A	-11.4	*Streptomyces* sp. KY002
CNP0343875	Chrodrimanin L	-11.4	*Penicillium* sp. SCS-KFD09
CNP0324082	Bisrubescensin A	-11.3	*Isodon rubescens*

Hits were filtered to exclude those with no explicit name. Affinity is given as the average binding affinity of heme to HO-1 chain A and chain B.

Supplemental Table 3. Top 20 hits from novel compound virtual screens.

Top 20 Competitive		Top 20 Selective	
Compound Number	BA (kcal/mol)	Compound Number	D (kcal/mol)
71	-12.45	71	16.5
63	-11.25	75	10.4
41	-10.8	106	7.35
106	-10.8	10	5.45
111	-10.5	68	2.9
51	-10.4	110	2.65
88	-10.4	58	1.9
92	-10.4	107	1.3
109	-10.35	37	0.9
79	-10.35	19	0.75
62	-10.25	17	0.55
25	-10.2	97	0.2
40	-10.2	1	-1.05
87	-10.2	42	-1.35
89	-10.2	63	-1.4
74	-10.15	48	-1.5
21	-10.15	109	-1.65
23	-10.15	113	-2.5
75	-10.15	35	-2.65
84	-10.15	114	-3

Competitiveness indicates high binding affinity (BA) of heme to HO-1. Affinity is given as the average binding affinity of heme to HO-1 chain A and chain B. Selectivity indicates a high difference in the binding affinity sum of heme to hemoproteins from heme to HO-1 (D). Each hemoprotein is normalized for its heme binding affinity and normalized to the binding affinity of heme to HO-1.

REFERENCES

1. Ritchie, H., Spooner, F., and Roser, M. (**2018**) Causes of death, *Our world in data*.

2. StatisticsCanada. (**2023**) Canadian Vital Statistics - Death database (CVSD), *Statistics Canada*.

3. Canadian Cancer Statistics Advisory Committee in collaboration with the Canadian Cancer Society, S. C., and the Public Health Agency of Canada. (**2023**) Canadian Cancer Statistics, *2023*.

4. Radman-Livaja, M., and Rando, O. J. (**2010**) Nucleosome positioning: how is it established, and why does it matter?, *Developmental biology 339*, 258-266.

5. Neigeborn, L., and Carlson, M. (**1984**) Genes affecting the regulation of SUC2 gene expression by glucose repression in Saccharomyces cerevisiae, *Genetics 108*, 845-858.

6. Stern, M., Jensen, R., and Herskowitz, I. (**1984**) Five SWI genes are required for expression of the HO gene in yeast, *Journal of molecular biology 178*, 853-868.

7. Kwon, H., Imbalzano, A. N., Khavari, P. A., Kingston, R. E., and Green, M. R. (**1994**) Nucleosome disruption and enhancement of activator binding by a human SW1/SNF complex, *Nature 370*, 477-481.

8. Wilson, B. G., and Roberts, C. W. (**2011**) SWI/SNF nucleosome remodellers and cancer, *Nature Reviews Cancer 11*, 481-492.

9. Wang, X., Haswell, J. R., and Roberts, C. W. (**2014**) Molecular pathways: SWI/SNF (BAF) complexes are frequently mutated in cancer—mechanisms and potential therapeutic insights, *Clinical cancer research 20*, 21-27.

10. Khavari, P. A., Peterson, C. L., Tamkun, J. W., Mendel, D. B., and Crabtree, G. R. (**1993**) BRG1 contains a conserved domain of the SWI2/SNF2 family necessary for normal mitotic growth and transcription, *Nature 366*, 170-174.

11. Jancewicz, I., Siedlecki, J. A., Sarnowski, T. J., and Sarnowska, E. (**2019**) BRM: the core ATPase subunit of SWI/SNF chromatin-remodelling complex—a tumour suppressor or tumour-promoting factor?, *Epigenetics & chromatin 12*, 68.

12. Willis, M. S., Homeister, J. W., Rosson, G. B., Annayev, Y., Holley, D., Holly, S. P., Madden, V. J., Godfrey, V., Parise, L. V., and Bultman, S. J. (**2012**) Functional redundancy of SWI/SNF catalytic subunits in maintaining vascular endothelial cells in the adult heart, *Circulation research 111*, e111-e122.

13. Fernando, T. M., Piskol, R., Bainer, R., Sokol, E. S., Trabucco, S. E., Zhang, Q., Trinh, H., Maund, S., Kschonsak, M., and Chaudhuri, S. (**2020**) Functional characterization of SMARCA4 variants identified by targeted exome-sequencing of 131,668 cancer patients, *Nature communications 11*, 5551.

14. Roberts, C. W., and Orkin, S. H. (**2004**) The SWI/SNF complex—chromatin and cancer, *Nature Reviews Cancer 4*, 133-142.

15. Clapier, C. R., and Cairns, B. R. (**2009**) The biology of chromatin remodeling complexes, *Annual review of biochemistry 78*, 273-304.

16. Kim, B., Luo, Y., Zhan, X., Zhang, Z., Shi, X., Yi, J., Xuan, Z., and Wu, J. (**2021**) Neuronal activity-induced BRG1 phosphorylation regulates enhancer activation, *Cell reports 36*.

17. Haldar, S. M., and McKinsey, T. A. (**2014**) BET-ting on chromatin-based therapeutics for heart failure, *Journal of molecular and cellular cardiology 74*, 98-102.

18. Güneş, C., Paszkowski-Rogacz, M., Rahmig, S., Khattak, S., Camgöz, A., Wermke, M., Dahl, A., Bornhäuser, M., Waskow, C., and Buchholz, F. (**2019**) Comparative RNAi screens in isogenic human stem cells reveal SMARCA4 as a differential regulator, *Stem cell reports 12*, 1084-1098.

19. Indra, A. K., Dupé, V., Bornert, J.-M., Messaddeq, N., Yaniv, M., Mark, M., Chambon, P., and Metzger, D. (**2005**) Temporally controlled targeted somatic mutagenesis in embryonic surface ectoderm and fetal epidermal keratinocytes unveils two distinct developmental functions of BRG1 in limb morphogenesis and skin barrier formation.

20. He, S., Pirity, M. K., Wang, W.-L., Wolf, L., Chauhan, B. K., Cveklova, K., Tamm, E. R., Ashery-Padan, R., Metzger, D., and Nakai, A. (**2010**) Chromatin remodeling enzyme Brg1 is required for mouse lens fiber cell terminal differentiation and its denucleation, *Epigenetics & chromatin 3*, 1-20.

21. Peng, L., Li, J., Wu, J., Xu, B., Wang, Z., Giamas, G., Stebbing, J., and Yu, Z. (**2021**) A pan-cancer analysis of SMARCA4 alterations in human cancers, *Frontiers in immunology 12*, 762598.

22. Schoenfeld, A. J., Bandlamudi, C., Lavery, J. A., Montecalvo, J., Namakydoust, A., Rizvi, H., Egger, J., Concepcion, C. P., Paul, S., and Arcila, M. E. (**2020**) The genomic landscape of SMARCA4 alterations and associations with outcomes in patients with lung cancer, *Clinical Cancer Research 26*, 5701-5708.

23. Jelinic, P., Mueller, J. J., Olvera, N., Dao, F., Scott, S. N., Shah, R., Gao, J., Schultz, N., Gonen, M., and Soslow, R. A. (**2014**) Recurrent SMARCA4 mutations in small cell carcinoma of the ovary, *Nature genetics 46*, 424-426.

24. Ramos, P., Karnezis, A. N., Craig, D. W., Sekulic, A., Russell, M. L., Hendricks, W. P., Corneveaux, J. J., Barrett, M. T., Shumansky, K., and Yang, Y. (**2014**) Small cell carcinoma of the ovary, hypercalcemic type, displays frequent inactivating germline and somatic mutations in SMARCA4, *Nature genetics 46*, 427-429.

25. Witkowski, L., Carrot-Zhang, J., Albrecht, S., Fahiminiya, S., Hamel, N., Tomiak, E., Grynspan, D., Saloustros, E., Nadaf, J., and Rivera, B. (**2014**) Germline and somatic

SMARCA4 mutations characterize small cell carcinoma of the ovary, hypercalcemic type, *Nature genetics 46*, 438-443.

26. Karnezis, A. N., Wang, Y., Ramos, P., Hendricks, W. P., Oliva, E., D'Angelo, E., Prat, J., Nucci, M. R., Nielsen, T. O., and Chow, C. (**2016**) Dual loss of the SWI/SNF complex ATPases SMARCA4/BRG1 and SMARCA2/BRM is highly sensitive and specific for small cell carcinoma of the ovary, hypercalcaemic type, *The Journal of pathology 238*, 389-400.

27. Gamwell, L. F., Gambaro, K., Merziotis, M., Crane, C., Arcand, S. L., Bourada, V., Davis, C., Squire, J. A., Huntsman, D. G., and Tonin, P. N. (**2013**) Small cell ovarian carcinoma: genomic stability and responsiveness to therapeutics, *Orphanet journal of rare diseases 8*, 1-14.

28. Kaelin Jr, W. G. (**2005**) The concept of synthetic lethality in the context of anticancer therapy, *Nature reviews cancer 5*, 689-698.

29. Mense, S. M., and Zhang, L. (**2006**) Heme: a versatile signaling molecule controlling the activities of diverse regulators ranging from transcription factors to MAP kinases, *Cell research 16*, 681-692.

30. Gonciarz, R. L., Collisson, E. A., and Renslo, A. R. (**2021**) Ferrous iron-dependent pharmacology, *Trends in pharmacological sciences 42*, 7-18.

31. Chiabrando, D., Vinchi, F., Fiorito, V., Mercurio, S., and Tolosano, E. (**2014**) Heme in pathophysiology: a matter of scavenging, metabolism and trafficking across cell membranes, *Frontiers in pharmacology 5*, 61.

32. Winterbourn, C. C. (**1995**) Toxicity of iron and hydrogen peroxide: the Fenton reaction, *Toxicology letters 82*, 969-974.

33. Fenton, H. J. H. (**1894**) LXXIII.—Oxidation of tartaric acid in presence of iron, *Journal of the Chemical Society, Transactions 65*, 899-910.

34. Carlsen, C. U., Møller, J. K., and Skibsted, L. H. (**2005**) Heme-iron in lipid oxidation, *Coordination Chemistry Reviews 249*, 485-498.

35. Pethő, D., Hendrik, Z., Nagy, A., Beke, L., Patsalos, A., Nagy, L., Póliska, S., Méhes, G., Tóth, C., and Potor, L. (**2021**) Heme cytotoxicity is the consequence of endoplasmic reticulum stress in atherosclerotic plaque progression, *Scientific reports 11*, 10435.

36. Hedblom, A., Hejazi, S. M., Canesin, G., Choudhury, R., Hanafy, K. A., Csizmadia, E., Persson, J. L., and Wegiel, B. (**2019**) Heme detoxification by heme oxygenase-1 reinstates proliferative and immune balances upon genotoxic tissue injury, *Cell Death & Disease 10*, 72.

37. Weintraub, L. R., Weinstein, M. B., Huser, H.-J., and Rafal, S. (**1968**) Absorption of hemoglobin iron: the role of a heme-splitting substance in the intestinal mucosa, *The Journal of Clinical Investigation 47*, 531-539.

38. Tenhunen, R., Marver, H. S., and Schmid, R. (**1968**) The enzymatic conversion of heme to bilirubin by microsomal heme oxygenase, *Proceedings of the National Academy of Sciences 61*, 748-755.

39. Tenhunen, R., Marver, H. S., and Schmid, R. (**1969**) Microsomal heme oxygenase: characterization of the enzyme, *Journal of Biological Chemistry 244*, 6388-6394.

40. Kumar, S., and Bandyopadhyay, U. (**2005**) Free heme toxicity and its detoxification systems in human, *Toxicology letters 157*, 175-188.

41. Kikuchi, G., Yoshida, T., and Noguchi, M. (**2005**) Heme oxygenase and heme degradation, *Biochemical and biophysical research communications 338*, 558-567.

42. Stocker, R., Yamamoto, Y., McDonagh, A. F., Glazer, A. N., and Ames, B. N. (**1987**) Bilirubin is an antioxidant of possible physiological importance, *Science 235*, 1043-1046.

43. Jansen, T., Hortmann, M., Oelze, M., Opitz, B., Steven, S., Schell, R., Knorr, M., Karbach, S., Schuhmacher, S., and Wenzel, P. (**2010**) Conversion of biliverdin to bilirubin by biliverdin reductase contributes to endothelial cell protection by heme oxygenase-1—evidence for direct and indirect antioxidant actions of bilirubin, *Journal of molecular and cellular cardiology 49*, 186-195.

44. Barañano, D. E., Rao, M., Ferris, C. D., and Snyder, S. H. (**2002**) Biliverdin reductase: a major physiologic cytoprotectant, *Proceedings of the national academy of sciences 99*, 16093-16098.

45. Kim, H. P., Wang, X., Zhang, J., Suh, G. Y., Benjamin, I. J., Ryter, S. W., and Choi, A. M. (**2005**) Heat shock protein-70 mediates the cytoprotective effect of carbon monoxide: involvement of p38β MAPK and heat shock factor-1, *The Journal of Immunology 175*, 2622-2629.

46. Chin, B. Y., Jiang, G., Wegiel, B., Wang, H. J., MacDonald, T., Zhang, X. C., Gallo, D., Cszimadia, E., Bach, F. H., and Lee, P. J. (**2007**) Hypoxia-inducible factor 1α stabilization by carbon monoxide results in cytoprotective preconditioning, *Proceedings of the National Academy of Sciences 104*, 5109-5114.

47. Conti, C. S. (**2021**) Bilirubin: the toxic mechanisms of an antioxidant molecule, *Arch Argent Pediatr 119*, e18-e25.

48. Zuckerbraun, B. S., Chin, B. Y., Bilban, M., d'Avila, J. d. C., Rao, J., Billiar, T. R., and Otterbein, L. E. (**2007**) Carbon monoxide signals via inhibition of cytochrome c oxidase and generation of mitochondrial reactive oxygen species, *The FASEB Journal 21*, 1099-1106.

49. Dixon, S. J., Lemberg, K. M., Lamprecht, M. R., Skouta, R., Zaitsev, E. M., Gleason, C. E., Patel, D. N., Bauer, A. J., Cantley, A. M., and Yang, W. S. (**2012**) Ferroptosis: an iron-dependent form of nonapoptotic cell death, *cell 149*, 1060-1072.

50. Maines, M. D., Trakshel, G., and Kutty, R. K. (**1986**) Characterization of two constitutive forms of rat liver microsomal heme oxygenase. Only one molecular species of the enzyme is inducible, *Journal of Biological Chemistry 261*, 411-419.

51. Alam, J., Shibahara, S., and Smith, A. (**1989**) Transcriptional activation of the heme oxygenase gene by heme and cadmium in mouse hepatoma cells, *Journal of Biological Chemistry 264*, 6371-6375.

52. Keyse, S. M., and Tyrrell, R. M. (**1989**) Heme oxygenase is the major 32-kDa stress protein induced in human skin fibroblasts by UVA radiation, hydrogen peroxide, and sodium arsenite, *Proceedings of the National Academy of Sciences 86*, 99-103.

53. Kochert, B. A., Fleischhacker, A. S., Wales, T. E., Becker, D. F., Engen, J. R., and Ragsdale, S. W. (**2019**) Dynamic and structural differences between heme oxygenase-1 and-2 are due to differences in their C-terminal regions, *Journal of Biological Chemistry 294*, 8259-8272.

54. Sun, J., Loehr, T. M., Wilks, A., and Ortiz de Montellano, P. R. (**1994**) Identification of histidine 25 as the heme ligand in human liver heme oxygenase, *Biochemistry 33*, 13734-13740.

55. Liu, Y., Moënne-Loccoz, P., Hildebrand, D. P., Wilks, A., Loehr, T. M., Mauk, A. G., and Ortiz de Montellano, P. R. (**1999**) Replacement of the proximal histidine iron ligand by a cysteine or tyrosine converts heme oxygenase to an oxidase, *Biochemistry 38*, 3733-3743.

56. Lightning, L. K., Huang, H.-w., Moënne-Loccoz, P., Loehr, T. M., Schuller, D. J., Poulos, T. L., and De Montellano, P. R. O. (**2001**) Disruption of an active site hydrogen bond converts human heme oxygenase-1 into a peroxidase, *Journal of Biological Chemistry 276*, 10612-10619.

57. Hwang, H.-W., Lee, J.-R., Chou, K.-Y., Suen, C.-S., Hwang, M.-J., Chen, C., Shieh, R.-C., and Chau, L.-Y. (**2009**) Oligomerization is crucial for the stability and function of heme oxygenase-1 in the endoplasmic reticulum, *Journal of Biological Chemistry 284*, 22672-22679.

58. Gottlieb, Y., Truman, M., Cohen, L. A., Leichtmann-Bardoogo, Y., and Meyron-Holtz, E. G. (**2012**) Endoplasmic reticulum anchored heme-oxygenase 1 faces the cytosol, *Haematologica 97*, 1489.

59. Huber, W. J., and Backes, W. L. (**2007**) Expression and characterization of full-length human heme oxygenase-1: the presence of intact membrane-binding region leads to increased binding affinity for NADPH cytochrome P450 reductase, *Biochemistry 46*, 12212-12219.

60. Na, H.-K., and Surh, Y.-J. (**2014**) Oncogenic potential of Nrf2 and its principal target protein heme oxygenase-1, *Free Radical Biology and Medicine 67*, 353-365.

61. Itoh, K., Wakabayashi, N., Katoh, Y., Ishii, T., Igarashi, K., Engel, J. D., and Yamamoto, M. (**1999**) Keap1 represses nuclear activation of antioxidant responsive elements by Nrf2 through binding to the amino-terminal Neh2 domain, *Genes & development 13*, 76-86.

62. Lee, J.-S., and Surh, Y.-J. (**2005**) Nrf2 as a novel molecular target for chemoprevention, *Cancer letters 224*, 171-184.

63. Ogawa, K., Sun, J., Taketani, S., Nakajima, O., Nishitani, C., Sassa, S., Hayashi, N., Yamamoto, M., Shibahara, S., and Fujita, H. (**2001**) Heme mediates derepression of Maf recognition element through direct binding to transcription repressor Bach1, *The EMBO journal 20*, 2835-2843.

64. Lee, P. J., Jiang, B.-H., Chin, B. Y., Iyer, N. V., Alam, J., Semenza, G. L., and Choi, A. K. (**1997**) Hypoxia-inducible factor-1 mediates transcriptional activation of the heme oxygenase-1 gene in response to hypoxia, *Journal of Biological Chemistry 272*, 5375-5381.

65. Lavrovsky, Y., Schwartzman, M. L., Levere, R. D., Kappas, A., and Abraham, N. G. (**1994**) Identification of binding sites for transcription factors NF-kappa B and AP-2 in the promoter region of the human heme oxygenase 1 gene, *Proceedings of the National Academy of Sciences 91*, 5987-5991.

66. Lin, C.-C., Chiang, L.-L., Lin, C.-H., Shih, C.-H., Liao, Y.-T., Hsu, M.-J., and Chen, B.-C. (**2007**) Transforming growth factor-β1 stimulates heme oxygenase-1 expression via the PI3K/Akt and NF-κB pathways in human lung epithelial cells, *European journal of pharmacology 560*, 101-109.

67. Wu, J., Li, S., Li, C., Cui, L., Ma, J., and Hui, Y. (**2021**) The non-canonical effects of heme oxygenase-1, a classical fighter against oxidative stress, *Redox Biology 47*, 102170.

68. Kim, H. P., Wang, X., Galbiati, F., Ryter, S. W., and Choi, A. M. (**2004**) Caveolae compartmentalization of heme oxygenase-1 in endothelial cells, *The FASEB Journal 18*, 1080-1089.

69. Slebos, D.-J., Ryter, S. W., Van Der Toorn, M., Liu, F., Guo, F., Baty, C. J., Karlsson, J. M., Watkins, S. C., Kim, H. P., and Wang, X. (**2007**) Mitochondrial localization and function of heme oxygenase-1 in cigarette smoke–induced cell death, *American journal of respiratory cell and molecular biology 36*, 409-417.

70. Lin, Q., Weis, S., Yang, G., Weng, Y.-H., Helston, R., Rish, K., Smith, A., Bordner, J., Polte, T., and Gaunitz, F. (**2007**) Heme oxygenase-1 protein localizes to the nucleus and activates transcription factors important in oxidative stress, *Journal of Biological Chemistry 282*, 20621-20633.

71. Bansal, S., Biswas, G., and Avadhani, N. G. (**2014**) Mitochondria-targeted heme oxygenase-1 induces oxidative stress and mitochondrial dysfunction in macrophages, kidney fibroblasts and in chronic alcohol hepatotoxicity, *Redox biology 2*, 273-283.

72. Bian, C., Zhong, M., Nisar, M. F., Wu, Y., Ouyang, M., Bartsch, J. W., and Zhong, J. L. (**2018**) A novel heme oxygenase-1 splice variant, 14kDa HO-1, promotes cell proliferation and increases relative telomere length, *Biochemical and biophysical research communications 500*, 429-434.

73. Hori, R., Kashiba, M., Toma, T., Yachie, A., Goda, N., Makino, N., Soejima, A., Nagasawa, T., Nakabayashi, K., and Suematsu, M. (**2002**) Gene transfection of H25A mutant heme oxygenase-1 protects cells against hydroperoxide-induced cytotoxicity, *Journal of Biological Chemistry 277*, 10712-10718.

74. Lin, Q. S., Weis, S., Yang, G., Zhuang, T., Abate, A., and Dennery, P. A. (**2008**) Catalytic inactive heme oxygenase-1 protein regulates its own expression in oxidative stress, *Free Radical Biology and Medicine 44*, 847-855.

75. Huppert, J. L., and Balasubramanian, S. (**2007**) G-quadruplexes in promoters throughout the human genome, *Nucleic acids research 35*, 406-413.

76. Lipps, H. J., and Rhodes, D. (**2009**) G-quadruplex structures: in vivo evidence and function, *Trends in cell biology 19*, 414-422.

77. Spiegel, J., Adhikari, S., and Balasubramanian, S. (**2020**) The structure and function of DNA G-quadruplexes, *Trends in Chemistry 2*, 123-136.

78. Lerner, L. K., and Sale, J. E. (**2019**) Replication of G quadruplex DNA, *Genes 10*, 95.

79. Rodriguez, R., Miller, K. M., Forment, J. V., Bradshaw, C. R., Nikan, M., Britton, S., Oelschlaegel, T., Xhemalce, B., Balasubramanian, S., and Jackson, S. P. (**2012**) Small-molecule–induced DNA damage identifies alternative DNA structures in human genes, *Nature chemical biology 8*, 301-310.

80. Xu, H., Di Antonio, M., McKinney, S., Mathew, V., Ho, B., O'Neil, N. J., Santos, N. D., Silvester, J., Wei, V., and Garcia, J. (**2017**) CX-5461 is a DNA G-quadruplex stabilizer with selective lethality in BRCA1/2 deficient tumours, *Nature communications 8*, 14432.

81. Li, C., Yin, Z., Xiao, R., Huang, B., Cui, Y., Wang, H., Xiang, Y., Wang, L., Lei, L., and Ye, J. (**2022**) G-quadruplexes sense natural porphyrin metabolites for regulation of gene transcription and chromatin landscapes, *Genome Biology 23*, 1-29.

82. Canesin, G., Muralidharan, A. M., Swanson, K. D., and Wegiel, B. (**2021**) HO-1 and Heme: G-Quadruplex interaction choreograph DNA damage responses and cancer growth, *Cells 10*, 1801.

83. Campbell, N. K., Fitzgerald, H. K., and Dunne, A. (**2021**) Regulation of inflammation by the antioxidant haem oxygenase 1, *Nature Reviews Immunology 21*, 411-425.

84. Idriss, N. K., Blann, A. D., and Lip, G. Y. (**2008**) Hemoxygenase-1 in cardiovascular disease, *Journal of the American College of Cardiology 52*, 971-978.

85. Ryter, S. W. (**2022**) Heme oxygenase-1: an anti-inflammatory effector in cardiovascular, lung, and related metabolic disorders, *Antioxidants 11*, 555.

86. Schipper, H. M. (**2004**) Heme oxygenase expression in human central nervous system disorders, *Free Radical Biology and Medicine 37*, 1995-2011.

87. Nitti, M., Piras, S., Marinari, U. M., Moretta, L., Pronzato, M. A., and Furfaro, A. L. (**2017**) HO-1 induction in cancer progression: a matter of cell adaptation, *Antioxidants 6*, 29.

88. Hahn, D., Shin, S. H., and Bae, J.-S. (**2020**) Natural antioxidant and anti-inflammatory compounds in foodstuff or medicinal herbs inducing heme oxygenase-1 expression, *Antioxidants 9*, 1191.

89. Woo, J., Iyer, S., Cornejo, M.-C., Mori, N., Gao, L., Sipos, I., Maines, M., and Buelow, R. (**1998**) Stress protein-induced immunosuppression: inhibition of cellular immune effector functions following overexpression of haem oxygenase (HSP 32), *Transplant immunology 6*, 84-93.

90. Zhang, A., Suzuki, T., Adachi, S., Naganuma, E., Suzuki, N., Hosoya, T., Itoh, K., Sporn, M. B., and Yamamoto, M. (**2021**) Distinct regulations of HO-1 gene expression for stress response and substrate induction, *Molecular and cellular biology 41*, e00236-00221.

91. Brouard, S., Otterbein, L. E., Anrather, J., Tobiasch, E., Bach, F. H., Choi, A. M., and Soares, M. P. (**2000**) Carbon monoxide generated by heme oxygenase 1 suppresses endothelial cell apoptosis, *The Journal of experimental medicine 192*, 1015-1026.

92. Fujita, T., Toda, K., Karimova, A., Yan, S.-F., Naka, Y., Yet, S.-F., and Pinsky, D. J. (**2001**) Paradoxical rescue from ischemic lung injury by inhaled carbon monoxide driven by derepression of fibrinolysis, *Nature medicine 7*, 598-604.

93. Motterlini, R., Clark, J. E., Foresti, R., Sarathchandra, P., Mann, B. E., and Green, C. J. (**2002**) Carbon monoxide-releasing molecules: characterization of biochemical and vascular activities, *Circulation research 90*, e17-e24.

94. Adach, W., Błaszczyk, M., and Olas, B. (**2020**) Carbon monoxide and its donors-Chemical and biological properties, *Chemico-biological interactions 318*, 108973.

95. Motterlini, R., and Otterbein, L. E. (**2010**) The therapeutic potential of carbon monoxide, *Nature reviews Drug discovery 9*, 728-743.

96. Vo, T. T. T., Vo, Q. C., Tuan, V. P., Wee, Y., Cheng, H.-C., and Lee, I.-T. (**2021**) The potentials of carbon monoxide-releasing molecules in cancer treatment: An outlook from ROS biology and medicine, *Redox Biology 46*, 102124.

97. Bauer, N., Yuan, Z., Yang, X., and Wang, B. (**2023**) Plight of CORMs: the unreliability of four commercially available CO-releasing molecules, CORM-2, CORM-3, CORM-A1, and CORM-401, in studying CO biology, *Biochemical Pharmacology*, 115642.

98. García-Gallego, S., and Bernardes, G. J. (**2014**) Carbon-monoxide-releasing molecules for the delivery of therapeutic CO in vivo, *Angewandte Chemie International Edition 53*, 9712-9721.

99. Zhao, Z., Xu, Y., Lu, J., Xue, J., and Liu, P. (**2018**) High expression of HO-1 predicts poor prognosis of ovarian cancer patients and promotes proliferation and aggressiveness of ovarian cancer cells, *Clinical and Translational Oncology 20*, 491-499.

100. Kim, H.-R., Kim, S., Kim, E.-J., Park, J.-H., Yang, S.-H., Jeong, E.-T., Park, C., Youn, M.-J., So, H.-S., and Park, R. (**2008**) Suppression of Nrf2-driven heme oxygenase-1 enhances the chemosensitivity of lung cancer A549 cells toward cisplatin, *Lung cancer 60*, 47-56.

101. Zhao, Z., Zhao, J., Xue, J., Zhao, X., and Liu, P. (**2016**) Autophagy inhibition promotes epithelial-mesenchymal transition through ROS/HO-1 pathway in ovarian cancer cells, *American journal of cancer research 6*, 2162.

102. Degese, M. S., Mendizabal, J. E., Gandini, N. A., Gutkind, J. S., Molinolo, A., Hewitt, S. M., Curino, A. C., Coso, O. A., and Facchinetti, M. M. (**2012**) Expression of heme oxygenase-1 in non-small cell lung cancer (NSCLC) and its correlation with clinical data, *Lung Cancer 77*, 168-175.

103. Labbé, R. F., Vreman, H. J., and Stevenson, D. K. (**1999**) Zinc protoporphyrin: a metabolite with a mission, *Clinical chemistry 45*, 2060-2072.

104. Maines, M. D. (**1981**) Zinc· protoporphyrin is a selective inhibitor of heme oxygenase activity in the neonatal rat, *Biochimica et Biophysica Acta (BBA)-General Subjects 673*, 339-350.

105. Fang, J., Sawa, T., Akaike, T., Akuta, T., Sahoo, S. K., Khaled, G., Hamada, A., and Maeda, H. (**2003**) In vivo antitumor activity of pegylated zinc protoporphyrin: targeted inhibition of heme oxygenase in solid tumor, *Cancer Research 63*, 3567-3574.

106. Fang, J., Sawa, T., Akaike, T., Greish, K., and Maeda, H. (**2004**) Enhancement of chemotherapeutic response of tumor cells by a heme oxygenase inhibitor, pegylated zinc protoporphyrin, *International journal of cancer 109*, 1-8.

107. Hirai, K., Sasahira, T., Ohmori, H., Fujii, K., and Kuniyasu, H. (**2007**) Inhibition of heme oxygenase-1 by zinc protoporphyrin IX reduces tumor growth of LL/2 lung cancer in C57BL mice, *International Journal of Cancer 120*, 500-505.

108. Maines, M. D. (**1988**) Heme oxygenase: function, multiplicity, regulatory mechanisms, and clinical applications, *The FASEB journal 2*, 2557-2568.

109. La, P., Fernando, A. P., Wang, Z., Salahudeen, A., Yang, G., Lin, Q., Wright, C. J., and Dennery, P. A. (**2009**) Zinc protoporphyrin regulates cyclin D1 expression independent of heme oxygenase inhibition, *Journal of Biological Chemistry 284*, 36302-36311.

110. Wang, S., Avery, J. E., Hannafon, B. N., Lind, S. E., and Ding, W.-Q. (**2013**) Zinc protoporphyrin suppresses cancer cell viability through a heme oxygenase-1-independent mechanism: The involvement of the Wnt/β-catenin signaling pathway, *Biochemical pharmacology 85*, 1611-1618.

111. Yang, G., Nguyen, X., Ou, J., Rekulapelli, P., Stevenson, D. K., and Dennery, P. A. (**2001**) Unique effects of zinc protoporphyrin on HO-1 induction and apoptosis, *Blood, The Journal of the American Society of Hematology 97*, 1306-1313.

112. Kwok, S. (**2013**) Zinc protoporphyrin upregulates heme oxygenase-1 in PC-3 cells via the stress response pathway, *International journal of cell biology 2013*.

113. Appleton, S. D., Chretien, M. L., McLaughlin, B. E., Vreman, H. J., Stevenson, D. K., Brien, J. F., Nakatsu, K., Maurice, D. H., and Marks, G. S. (**1999**) Selective inhibition of heme oxygenase, without inhibition of nitric oxide synthase or soluble guanylyl cyclase, by metalloporphyrins at low concentrations, *Drug metabolism and disposition 27*, 1214-1219.

114. Wong, R., Vreman, H., Schulz, S., Kalish, F., Pierce, N., and Stevenson, D. (**2011**) In vitro inhibition of heme oxygenase isoenzymes by metalloporphyrins, *Journal of perinatology 31*, S35-S41.

115. Vlahakis, J. Z., Kinobe, R. T., Bowers, R. J., Brien, J. F., Nakatsu, K., and Szarek, W. A. (**2005**) Synthesis and evaluation of azalanstat analogues as heme oxygenase inhibitors, *Bioorganic & medicinal chemistry letters 15*, 1457-1461.

116. Sorrenti, V., Guccione, S., Di Giacomo, C., Modica, M. N., Pittalà, V., Acquaviva, R., Basile, L., Pappalardo, M., and Salerno, L. (**2012**) Evaluation of imidazole-based compounds as heme oxygenase-1 inhibitors, *Chemical Biology & Drug Design 80*, 876-886.

117. Salerno, L., Pittalà, V., Romeo, G., Modica, M. N., Siracusa, M. A., Di Giacomo, C., Acquaviva, R., Barbagallo, I., Tibullo, D., and Sorrenti, V. (**2013**) Evaluation of novel aryloxyalkyl derivatives of imidazole and 1, 2, 4-triazole as heme oxygenase-1 (HO-1) inhibitors and their antitumor properties, *Bioorganic & medicinal chemistry 21*, 5145-5153.

118. Floresta, G., Pittala, V., Sorrenti, V., Romeo, G., Salerno, L., and Rescifina, A. (**2018**) Development of new HO-1 inhibitors by a thorough scaffold-hopping analysis, *Bioorganic Chemistry 81*, 334-339.

119. Salerno, L., Amata, E., Romeo, G., Marrazzo, A., Prezzavento, O., Floresta, G., Sorrenti, V., Barbagallo, I., Rescifina, A., and Pittalà, V. (**2018**) Potholing of the hydrophobic heme oxygenase-1 western region for the search of potent and selective imidazole-based inhibitors, *European Journal of Medicinal Chemistry 148*, 54-62.

120. Ciaffaglione, V., Intagliata, S., Pittalà, V., Marrazzo, A., Sorrenti, V., Vanella, L., Rescifina, A., Floresta, G., Sultan, A., and Greish, K. (**2020**) New arylethanolimidazole derivatives as HO-1 inhibitors with cytotoxicity against MCF-7 breast cancer cells, *International Journal of Molecular Sciences 21*, 1923.

121. Fallica, A. N., Sorrenti, V., D'Amico, A. G., Salerno, L., Romeo, G., Intagliata, S., Consoli, V., Floresta, G., Rescifina, A., and D'Agata, V. (**2021**) Discovery of novel acetamide-based heme Oxygenase-1 inhibitors with potent in vitro antiproliferative activity, *Journal of Medicinal Chemistry 64*, 13373-13393.

122. Subashini, G., Vidhya, K., Arasakumar, T., Angayarkanni, J., Murugesh, E., Saravanan, A., Shanmughavel, P., and Mohan, P. S. (**2018**) Quinoline-Based Imidazole Derivative as Heme Oxygenase-1 Inhibitor: A Strategy for Cancer Treatment, *ChemistrySelect 3*, 3680-3686.

123. Salerno, L., Pittala, V., Romeo, G., Modica, M. N., Marrazzo, A., Siracusa, M. A., Sorrenti, V., Di Giacomo, C., Vanella, L., and Parayath, N. N. (**2015**) Novel imidazole derivatives as heme oxygenase-1 (HO-1) and heme oxygenase-2 (HO-2) inhibitors and their cytotoxic activity in human-derived cancer cell lines, *European Journal of Medicinal Chemistry 96*, 162-172.

124. Amata, E., Marrazzo, A., Dichiara, M., Modica, M. N., Salerno, L., Prezzavento, O., Nastasi, G., Rescifina, A., Romeo, G., and Pittalà, V. (**2017**) Heme oxygenase database (HemeOxDB) and QSAR analysis of isoform 1 inhibitors, *ChemMedChem 12*, 1873-1881.

125. Floresta, G., Amata, E., Gentile, D., Romeo, G., Marrazzo, A., Pittalà, V., Salerno, L., and Rescifina, A. (**2019**) Fourfold filtered statistical/computational approach for the identification of imidazole compounds as HO-1 inhibitors from natural products, *Marine Drugs 17*, 113.

126. Sun, B., Sun, Z., Jin, Q., and Chen, X. (**2008**) CO-releasing molecules (CORM-2)-liberated CO attenuates leukocytes infiltration in the renal tissue of thermally injured mice, *International Journal of Biological Sciences 4*, 176.

127. Trott, O., and Olson, A. J. (**2010**) AutoDock Vina: improving the speed and accuracy of docking with a new scoring function, efficient optimization, and multithreading, *Journal of computational chemistry 31*, 455-461.

128. Eberhardt, J., Santos-Martins, D., Tillack, A. F., and Forli, S. (**2021**) AutoDock Vina 1.2. 0: New docking methods, expanded force field, and python bindings, *Journal of chemical information and modeling 61*, 3891-3898.

129. Sterling, T., and Irwin, J. J. (**2015**) ZINC 15–ligand discovery for everyone, *Journal of chemical information and modeling 55*, 2324-2337.

130. Sorokina, M., Merseburger, P., Rajan, K., Yirik, M. A., and Steinbeck, C. (**2021**) COCONUT online: collection of open natural products database, *Journal of Cheminformatics 13*, 1-13.

131. Enamine. (2023) Enamine REAL compounds, https://enamine.net/library-synthesis/real-compounds.

132. Morris, G. M., Huey, R., Lindstrom, W., Sanner, M. F., Belew, R. K., Goodsell, D. S., and Olson, A. J. (**2009**) AutoDock4 and AutoDockTools4: Automated docking with selective receptor flexibility, *Journal of computational chemistry 30*, 2785-2791.

133. Gorgulla, C., Boeszoermenyi, A., Wang, Z.-F., Fischer, P. D., Coote, P. W., Padmanabha Das, K. M., Malets, Y. S., Radchenko, D. S., Moroz, Y. S., and Scott, D. A. (**2020**) An open-source drug discovery platform enables ultra-large virtual screens, *Nature 580*, 663-668.

134. Feinstein, W. P., and Brylinski, M. (**2015**) Calculating an optimal box size for ligand docking and virtual screening against experimental and predicted binding pockets, *Journal of cheminformatics 7*, 1-10.

135. Gueron, G., Giudice, J., Valacco, P., Paez, A., Elguero, B., Toscani, M., Jaworski, F., Leskow, F. C., Cotignola, J., and Marti, M. (**2014**) Heme-oxygenase-1 implications in cell morphology and the adhesive behavior of prostate cancer cells, *Oncotarget 5*, 4087.

136. Chen, X., Wei, S.-Y., Li, J.-S., Zhang, Q.-F., Wang, Y.-X., Zhao, S.-L., Yu, J., Wang, C., Qin, Y., and Wei, Q.-J. (**2016**) Overexpression of heme oxygenase-1 prevents renal interstitial inflammation and fibrosis induced by unilateral ureter obstruction, *PloS one 11*, e0147084.

137. Walters, W. P., Stahl, M. T., and Murcko, M. A. (**1998**) Virtual screening—an overview, *Drug discovery today 3*, 160-178.

138. Song, S., Nguyen, V., Schrank, T., Mulvaney, K., Walter, V., Wei, D., Orvis, T., Desai, N., Zhang, J., and Hayes, D. N. (**2020**) Loss of SWI/SNF chromatin remodeling alters NRF2 signaling in Non–small cell lung carcinoma, *Molecular Cancer Research 18*, 1777-1788.

139. Kuo, L. J., and Yang, L.-X. (**2008**) γ-H2AX-a novel biomarker for DNA double-strand breaks, *In vivo 22*, 305-309.

140. Munari, C. C., de Oliveira, P. F., Campos, J. C. L., Martins, S. d. P. L., Da Costa, J. C., Bastos, J. K., and Tavares, D. C. (**2014**) Antiproliferative activity of Solanum lycocarpum alkaloidic extract and their constituents, solamargine and solasonine, in tumor cell lines, *Journal of natural medicines 68*, 236-241.

141. Gao, J., Song, L., Xia, H., Peng, L., and Wen, Z. (**2020**) 6′-O-galloylpaeoniflorin regulates proliferation and metastasis of non-small cell lung cancer through AMPK/miR-299-5p/ATF2 axis, *Respiratory Research 21*, 1-15.

142. Jin, M., Shi, C., Li, T., Wu, Y., Hu, C., and Huang, G. (**2020**) Solasonine promotes ferroptosis of hepatoma carcinoma cells via glutathione peroxidase 4-induced destruction of the glutathione redox system, *Biomedicine & Pharmacotherapy 129*, 110282.

143. Ewing, J. F., and Maines, M. D. (**1993**) Glutathione depletion induces heme oxygenase-1 (HSP32) mRNA and protein in rat brain, *Journal of neurochemistry 60*, 1512-1519.

144. Rogers, D. M., Agarwal, R., Vermaas, J. V., Smith, M. D., Rajeshwar, R. T., Cooper, C., Sedova, A., Boehm, S., Baker, M., and Glaser, J. (**2023**) SARS-CoV2 billion-compound docking, *Scientific Data 10*, 173.

145. Gorgulla, C., Nigam, A., Koop, M., Cinaroglu, S. S., Secker, C., Haddadnia, M., Kumar, A., Malets, Y., Hasson, A., and Levin-Konigsberg, R. (**2023**) VirtualFlow 2.0-The Next Generation Drug Discovery Platform Enabling Adaptive Screens of 69 Billion Molecules, *bioRxiv*, 2023.2004. 2025.537981.

146. Ryter, S. W., Alam, J., and Choi, A. M. (**2006**) Heme oxygenase-1/carbon monoxide: from basic science to therapeutic applications, *Physiological reviews 86*, 583-650.

147. Knox, C., Wilson, M., Klinger, C. M., Franklin, M., Oler, E., Wilson, A., Pon, A., Cox, J., Chin, N. E., and Strawbridge, S. A. (**2024**) DrugBank 6.0: the DrugBank Knowledgebase for 2024, *Nucleic Acids Research 52*, D1265-D1275.